

Diese Arbeit hat begutachtet

.....



TECHNISCHE
UNIVERSITÄT
WIEN

Vienna University of Technology

DIPLOMARBEIT

Wet-Chemical-Synthesis and Pulsed-Field Studies of Magnetoelectric Composites

ausgeführt zum Zwecke der Erlangung des akademischen Grades eines
Diplom-Ingenieurs unter der Leitung von

Ao.Univ.Prof.i.R. Projektass. Univ.Prof. Dipl.-Ing.

Dr.techn.Roland Grössinger

E138 - Institut für Festkörperphysik

sowie

Ao.Univ.Prof. Univ.Prof. Dipl.-Ing. Dr.techn. Wolfgang Linert

E163 - Institut für angewandte Synthesechemie

eingereicht an der Technischen Universität Wien

Fakultät für Physik

von

Jakob Krippel

Matrikelnummer 0426710

Hintere Zollamtsstrasse 11/11, 1030 Wien

Wien, am 11.02.2015

Unterschrift

Kurzfassung

Die mögliche Kopplung von elektrischer Polarisierung und der Magnetisierung in magnetoelektrischen Materialien, hat enormes Interesse an derartigen Verbindungen innerhalb der letzten zwanzig Jahre ausgelöst. Die Kombination von ferroelektrischen und magnetischen Materialien in neuartigen Kompositverbindungen ermöglicht magnetoelektrisches Verhalten bei Raumtemperatur.

In dieser Arbeit werden magnetoelektrische Pulver-Komposite aus magnetostriktivem CoFe_2O_4 und piezoelektrischem BaTiO_3 bzw. CoFe_2O_4 und $\text{Pb}(\text{ZrTi})\text{O}_3$, hergestellt mittels verschiedener Sol-Gel-Synthesemethoden, präsentiert. Außerdem wird der Einfluss von chemischer Synthese und Produktionsparametern wie Stöchiometrie, Sinter- und Presskonditionen auf den magnetoelektrischen Koeffizienten und auf die Mikrostruktur der Verbindungen untersucht. Der Sol-Gel Prozess überzeugte im Vergleich mit herkömmlichen keramischen Methoden bzw. mechanischem Vermischen der Ausgangsstoffe durch das Erreichen einer homogenen Mikrostruktur, hoher Dichte und guter Verteilung von Ferrit- und PZT-Partikeln. Das Komposit mit der Zusammensetzung 55% Kobaltferrit und 45% PZT, gesintert bei 1000°C für zwei Stunden, erreichte den höchsten magnetoelektrischen Koeffizienten von $\alpha=2.97 \text{ mV}/(\text{cm}\cdot\text{Oe})$.

Eine neue Messmethode zur Charakterisierung magnetoelektrischer Verbindungen, bestehend aus einem magnetischen Pulsfeld und einem ladungssensitiven Verstärker, wurde ebenfalls entwickelt. Dieses Messverfahren ermöglicht eine direkte Messung der durch das Pulsfeld entstehenden elektrischen Ladung. Im Vergleich zur weit verbreiteten dynamischen Methode können hier Frequenzabhängigkeiten und Entladungsphänomene, die das Messergebnis beeinflussen, vermieden werden.

Abstract

The strong coupling of electric polarization and magnetization in magnetoelectric materials has attracted tremendous interest of researchers over the last 20 years. The unobstructed combination of ferroelectric and magnetostriuctive materials in composites allows magnetoelectric behavior even at room temperature.

In this work we present different sol-gel routines for bulk composites of magnetostriuctive CoFe_2O_4 and piezoelectric BaTiO_3 as well as CoFe_2O_4 and $\text{Pb}(\text{ZrTi})\text{O}_3$. We investigate the influence of chemical synthesis and production parameters such as stoichiometry, sintering and pressing conditions on the magnetoelectric coefficient. This offers new insights into the correlation of microstructure and magnetoelectricity. We found the sol-gel process most convincing through homogeneous microstructure, high density and efficient particle dispersion compared to conventional ceramic methods and mechanical mixing. A composition of 55% Cobalt Ferrite and 45% PZT, sintered at 1000°C for 2 hours, provided the maximum magnetoelectric response with $2.97 \text{ mV}/(\text{cm}\cdot\text{Oe})$.

Furthermore we present a novel measurement setup for composite characterization, combining a magnetic pulse field and a charge amplifier. This new method offers a direct approach of magnetoelectric measurement through processing electric charges caused by a magnetic pulse. Compared to the state-of-the art dynamic method, frequency dependencies and discharging processes do not occur and hence this new measurement setup will open new avenues for characterization of bulk ME materials.

Acknowledgement

First and foremost I would like to thank my advisers Prof. Roland Grössinger and Prof. Wolfgang Linert for giving me the opportunity to do scientific research in between Physics and Chemistry. Working in two disciplines provided diversified challenges during the course of this thesis. In addition to that they enabled my attendance to an international conference in New York and a cooperation with the group of Prof. Roman Boca at the TU Bratislava, which was thankfully supported by CENTROPE. I also enjoyed the lively discussions aside from scientific topics.

The financial support to the Austrian Science Foundation (FWF), project numbers S10406-N16 and 19335-N17 was gladly appreciated.

Special thanks also to Prof. Frank Kubel and Dipl.Ing. Maria Pantazi for their assistance in XRD-analysis and providing furnaces for sintering my samples. I thank Dr. Martin Kriegisch and Markus Schönhart for introducing me to the art of soldering and for supporting me during the design of the measurement setup. Together with Dr. Atif Muhammad I explored the field of magnetoelectric composites and our conversations were helpful during times when success seemed far away. Dr. Myrvete Tafili and Dr. Bashkim Misini offered their advice on chemical synthesis.

I owe deep gratitude to my wonderful parents for providing constant moral support and their patience with the duration of my studies. Their unconditional love and believe in me are the foundation upon which I live my life and I can't even try to express how lucky I am to have them. Together with my little sister Julia I am blessed to have a strong and supporting family, that always cares for each other.

I also want to mention my former roommates and friends David and

Lukas, who made my life as a student memorable and entertaining - “Zollamt”- forever.

In Dr. Franz Eder i met a great colleague that turned into a friend for life over the years.

Special thanks to Martin and Klemens (the circle of thrust), who have been my best friends for a very long time.

At the Basketball Club WAT Landstrasse Capricorns I found a second home. They softly pushed me into coaching a youth team which turned out to be my greatest passion. Thanks to Martin, Stano, Bedros, Günter and all the others especially, my U16/U19 boys team. Because of you I have no private life and finishing this thesis took forever but I wouldn't want to miss anything.

Finally I want to thank my beloved girlfriend Caroline for her constant support and also the acceptance of my Basketball-spleen. Thank you for sometimes pushing me into the right direction without even knowing it and for making me a better person every day.

Contents

1	Introduction	8
1.1	History of the ME Effect	8
1.2	Single-Phased Materials	9
1.2.1	Magnetically Induced Ferroelectricity	11
1.3	Magnetoelectric Composites	13
1.3.1	Types of ME Composites	16
1.3.2	Nanostructured Composite Thin Films	18
1.4	Applications	19
1.5	Objectives Of This Work	24
2	Measurement Technique	26
2.1	Methods For ME Characterization	26
2.2	The Pulse Field Method Utilizing a Charge Amplifier	29
2.2.1	The Charge Amplifier (Kistler 5001)	30
2.2.2	Operating the Charge Amplifier	31
2.2.3	Calibration of the Charge Amplifier	32
2.3	Discussion of Units of the ME effect	33
3	Experimental Procedures	36
3.1	Chemical Synthesis	36
3.1.1	Synthesis of CoFe_2O_4 via a nitrate-citrate gel combustion route	36
3.1.2	Synthesis of BaTiO_3 - CoFe_2O_4 Composites	37
3.1.2.1	Problems	38

3.1.3	Synthesis of CoFe_2O_4 -PZT composites by nitrate-citrate combustion	39
3.1.4	Pressing and Sintering	42
3.1.5	Thermogravimetric Analysis	42
3.1.6	Structural Analysis	43
3.1.7	Electric Poling	43
3.1.7.1	Problems	44
3.1.8	Magnetic Characterization	45
3.1.8.1	Analysis of magnetization measurement data	45
3.1.9	Magnetostriction Measurements	45
3.1.9.1	Analysis of Magnetostriction Measurement Data	47
3.1.10	Magnetoelectric Characterization	48
4	Results and Discussion	50
4.1	Composites of CoFe_2O_4 and BaTiO_3	50
4.1.1	CFBT_01-CFBT_03	50
4.1.2	CFBT_04-CFBT_07	52
4.1.3	Magnetoelectric Measurements	55
4.1.4	Magnetostriction and Magnetic Measurements	56
4.1.5	Conclusions	56
4.2	Composites of CoFe_2O_4 and PZT	58
4.2.1	XRD-Results	58
4.2.2	Scanning Electron Microscopy Analysis	61
4.2.3	Thermogravimetric Analysis	64
4.2.4	Magnetic Measurements	65
4.2.5	Magnetostriction	67
4.2.6	Magnetoelectric Effect in $\text{CF}_x\text{PZT}_{1-x}$ Composites	70
4.3	Effect of processing parameters on the ME coefficient	75
4.3.1	Magnetic and Magnetostriction Measurements	76
4.3.2	Magnetoelectric Measurements	77
4.3.3	Conclusions	79
4.4	Influence of phase connectivity on the ME effect	81
4.4.1	Structural Analysis and SEM studies	81

<i>CONTENTS</i>	<i>7</i>
4.4.2 Magnetic and Magnetoelectric Characterization	82
4.4.3 Conclusion	85
5 Conclusion and Outline	87
6 Scientific Activities	91

Chapter 1

Introduction: The Magnetoelectric Effect (ME) an Overview

1.1 History of the ME Effect

The magnetoelectric effect can be defined as the dielectric polarization of a material in an applied magnetic field ME_H - effect or as an induced magnetization in an external electric field ME_E effect [1]. Already at the beginning of the 19th century P. Curie introduced the possibility of an intrinsic ME behavior as a result of symmetry considerations [2]. The term magnetoelectric was suggested by Debye [3] decades after Curie mentioned his ideas. Dzyaloshinskii perpetuated the symmetry considerations of predecessors and explicitly predicted the possibility of the ME effect for Cr_2O_3 [4]. First successful experimental realization followed also in the early 1960's when magnetically induced polarization and electric-field induced magnetization were confirmed by Astrov and others in crystals of Cr_2O_3 [5] [6]. Below the antiferromagnetic Neel-temperature of 307 K ME effect peaked at $\alpha=4,13 \text{ ps m}^{-1}$. Despite the obvious breakthrough for ME research the relatively small magnitude of the ME effect in Cr_2O_3 as well as the required low temperatures prohibited possible technical applications. However the possibility of mutual control between

magnetic and electric order made further search for new magnetoelectric materials interesting.

About ten years after the first detection of the ME effect Van Suchtelen and others at the Philips Laboratories in the Netherlands tried to overcome that problem by combining magnetoelastic (piezomagnetic) and ferroelectric materials via strain mediation. Through unidirectional solidification they formed a eutectic composite of magnetostrictive CoFe_2O_4 and ferroelectric BaTiO_3 [7, 8]. Magnetoelectric voltage coefficients of up to $130 \text{ mV}/(\text{cm}\cdot\text{Oe})$ corresponding to $\alpha=720 \text{ ps m}^{-1}$ [9] outmatched performance of single phased materials by up to two orders of magnitude.

Despite the obvious success in ME research, it took until the 1990s when interest in new magnetoelectric materials rapidly started growing. New topics of interest related to ME interactions came up and modern experimental techniques as well as new theoretical concepts lead to a subsequent boom in magnetoelectric research over the last two decades shown in Fig. 1.1.1. The wide range of possible application of magnetoelectric materials as sensors, actuators, transducers, dual electric-field and magnetic-field tunable devices as well as memory devices drives scientists all over the world to find new substances and optimize respective magnetoelectric performance.

1.2 Single-Phased Materials

The term multiferroism has been introduced by Schmid [11] in order to describe materials showing the coexistence of either two or all three properties of ferroelectricity, ferromagnetism as well as ferroelasticity in a single phase. Magnetoelectricity per definition requires the first two of the mentioned. However the number of materials exhibiting a combination of those qualities is strongly limited for a various reasons.

A primary requirement for ferroelectricity is a structural distortion from a typically temperature dependent high symmetry phase that breaks spacial inversion. There are 31 point groups that allow spontaneous polarization \mathbf{P} . Spontaneous magnetization is invariant to spacial inversion however time reversal is not an allowed operation limiting the number of possible point

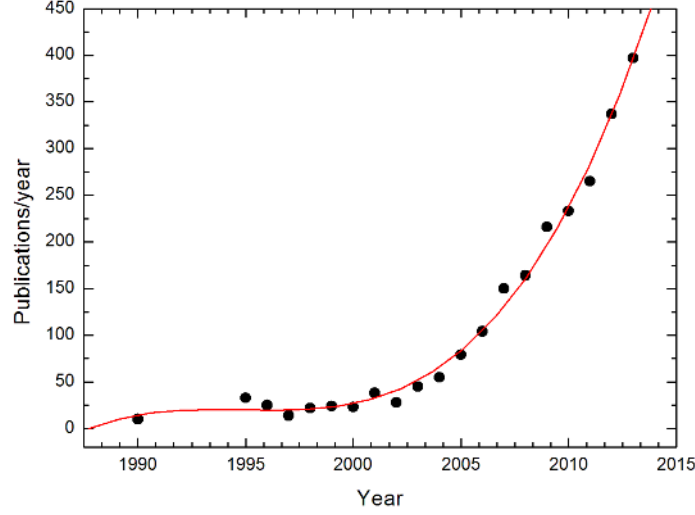


Figure 1.1.1: Publications per year with “magnetoelectric” as a keyword according to ScienceDirect [10]

groups also to 31. Overall thirteen point groups (of overall 122 Shubnikov point groups) allow the coexistence of both properties in the same phase.

Ferromagnetism has its microscopic origin in the presence of localized electrons, preferably in partially filled d- and f-orbitals of transition- and rare earth metals. These electrons show a locally corresponding spins and hence a magnetic moment. The interaction of those local magnetic moments enables a magnetic order. The direction of this spontaneous magnetization can be changed by application of an external field and above the Curie-temperature T_c overall magnetic order is lost, magnetic moments are oriented randomly and a paramagnetic behavior is the result.

Ferroelectricity per definition is the phase transition from a ordinary dielectric phase at high temperatures to a low temperature phase where polarization occurs spontaneously and its direction can be switched by an external electric field. Oxide structures with the chemical formula ABO_3 , see Fig. 1.2.1a), (A being an ion at the lattice corners, typically rare-earth or alkali metals, B being a small cation at the center of the lattice), called perovskites,

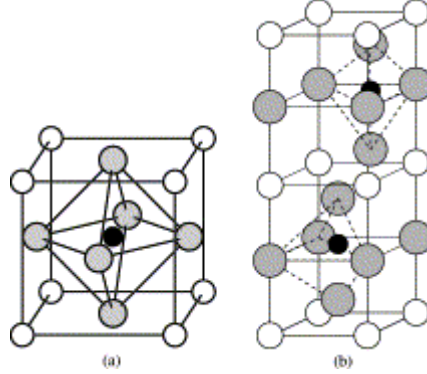


Figure 1.2.1: a) cubic perovskite structure . Small B-cation (black) in the center of an octahedron of oxygen anions (grey). Large A cations in the corners of the unit cell. b) hexagonal perovskite structure. The small B-cation is five-fold coordinated by oxygen anions [12]

for example BaTiO_3 , show such characteristic phase tranistions achieving spontaneous polarization through the off-center distortion of the cation. It is commonly believed that ferroelectricity in conventional perovskites is possible because of ligand field stabilization in which the formally filled oxygen 2p states donate electron density into the formally empty d-states of the transition metal cation as it moves off-center. In contrary to ferromagnetism vacant d-oribital states are required. This so called “ d^0 - d^n ” problem has been subject of intensive theoretical studies [12, 13].

Consequently a coexistence of ferroelectricity and ferromagnetism in a single phased material should be inconsisnt with mentioned theories. However up to the 1990s multiferroic behavior was found in about 80 compounds like Ti_2O_3 , GaFeO_3 , several boracite, and phosphate compounds, solid solituions like $\text{PbFe}_{0.5}\text{Nb}_{0.5}\text{O}_3$ summarized elsewhere [9].

1.2.1 Magnetically Induced Ferroelectricity

In recent years two classes of single phased multiferroic materials emerged. The first class is formed by materials, were a non centrosymmetric magnetic ordering breaks the inversion symmetry and induces a ferroelectric state. Therefore a those materials usually show a particularly strong magnetoelec-

tric coupling since the polarization is intimately coupled to magnetic ordering. Representatives of this class of magnetically induced multiferroism are orthorhombic TbMnO_3 or TbMn_2O_5 . Only the presence of a magnetic order enables spontaneous polarization. The strong coupling between magnetism and ferroelectricity appears by application of an external field which, in case of TbMnO_3 flips the direction of the polarization in a 90° angle, when applied in a certain direction [14]. In TbMn_2O_5 the effect is even stronger hence polarization changes sign with the external field and switching between -1,5 T and 1,5 T causes corresponding oscillations in the polarizations [15]. Magnetically induced polarization caused great excitement among researchers because of the unusual strong coupling of ferromagnetism and ferroelectricity. However such coupling requires low temperatures (for TbMnO_3 below $T = 30\text{K}$).

The second class is made of multiferroics where ferroelectric and magnetic order emerge independently. These were the first multiferroics discovered and a larger number of materials can be found among this class. Usually these types of multiferroics are good ferroelectrics and critical temperatures for magnetic and electric ordering are often above room temperature. Ferroelectricity is again the consequence of non-centrosymmetric structure and magnetic order occurs unrelated in different parts of the unit cell. Consequently the coupling between magnetism and ferroelectricity is rather weak and also a valid explanation for simultaneous existence of both properties has not yet been presented. Different mechanisms for multiferroic behavior within this class of materials have been identified and a small selection of them follows.

- Several ferroelectric perovskites show additional magnetic order despite the inconsistency with occupied and free d-orbitals in the transition metal. A way around the “ d^0 - d^n ” may be found through a formation of mixed perovskites with d^0 and d^n transition metals.
- The most prominent member of this class of multiferroics is BiFeO_3 . The Bi^{3+} ion plays a critical role in ferroelectricity. These ions possess two outer 6s electrons that do not participate in chemical bond. These

so called “lone pairs” have a high polarizability and on microscopic level the origin of ferroelectricity in these compounds can be explained by ordering of these lone pairs (with certain admixture of p orbitals) in one direction [16].

- YMnO_3 crystallizes in hexagonal perovskite structure shown in Fig. 1.2.1b). Ferroelectricity in YMnO_3 has nothing to do with magnetic Mn^{3+} but rather is a result of the tilting of MnO_5 block and a simultaneous shift from oxygen ions to the Y sites resulting in a change in respective bond-lengths and a subsequent polarization [17]

BiFeO_3 is the most intensively studied single phased multiferroic. The simple explanation lies within the very high ferroelectric Curie-temperature $T_c \sim 1103$ K as well as a high antiferromagnetic Neel-temperature $T_N \sim 643$ K, both well above room temperature and thus extremely interesting for possible applications. Ferroelectricity in BiFeO_3 has been known for a long time although its magnitude is much lower than in typical ferroelectric perovskites like BaTiO_3 or PZT.

BiFeO_3 shows classic antiferromagnetic behavior meaning neighbouring Fe-moments are aligned antiparallel. Those alignments are in fact not perfectly antiparallel, leaving a small canting moment. Investigations of BiFeO_3 thin films lead to very promising results in terms of enhanced ferroelectricity and stronger magnetoelectric coupling compared to bulk or even single crystal material [18]. The recently reported ferroelectric switching of antiferromagnetic domains in BiFeO_3 at room temperature, as a result of the respective reaction to an underlying ferroelastic domain structure [19], paves the way for extended discussion of approaching to control and switch magnetic properties by an electric field.

1.3 Magnetoelectric Composites

Parallel to the experiments with single-phased ME materials, the idea of combining two separate materials with either magnetostrictive or ferroelectric

properties in one composite found positive resonance. The physical properties of a material that is formed from two or more single-phased constituents depend both on the properties of the constituents and on the respective interaction between them. Combinations of two or more materials into a composite can result in three different effects [9] graphically shown in Fig. 1.3.1:

- Sum properties: the resulting effect is a weighted sum of the respective contributions from the original materials, the weight determined by the fraction of each constituent. Density or resistivity are examples for this kind of composite.
- Scaling or combination properties: the amplitude of the effect is higher for the composite than for the constituent materials meaning an enhancement of the average effect.
- Product properties: A new effect is present in the composite which is not represented in either one of the constituents. The fraction as well as the connectivity between the constituents determine the resulting effect.

Van Suchtelene et al. [7] were the first to propose and realize a combination of magnetostrictive and piezoelectric materials to obtain a magnetoelectric composite of magnetostrictive CoFe_2O_4 and ferroelectric BaTiO_3 . Although neither constituent shows ME behavior, the product properties of magnetostriction and piezoelectricity result in a magnetoelectric effect. Exposing the composite to a magnetic field induces a strain in the magnetostrictive material which is translated to the piezoelectric constituent, where it causes electric polarization.

The ME effect of this kind of composite can be written as [20]

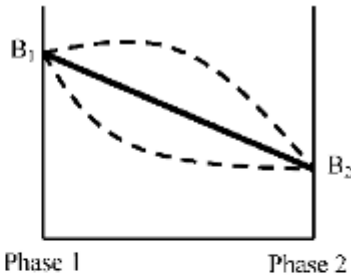
$$ME_E \text{ Effect} = \frac{\text{electrical}}{\text{mechanical}} \times \frac{\text{mechanical}}{\text{magnetic}}$$

or

$$ME_H \text{ Effect} = \frac{\text{magnetic}}{\text{mechanical}} \times \frac{\text{mechanical}}{\text{electric}}$$

(a) Sum Properties

Phase 1 : $A \rightarrow B_1$
Phase 2 : $A \rightarrow B_2$ $\bigcup A \rightarrow B^*$



(b) Product Properties

Phase 1 : $A \rightarrow B$
Phase 2 : $B \rightarrow C$ $\bigcup A \rightarrow C$ New Function

(c) Combination Properties

Phase 1 : $A \rightarrow B_1/C_1$
Phase 2 : $A \rightarrow B_2/C_2$ $\bigcup A \rightarrow (B/C)^*$

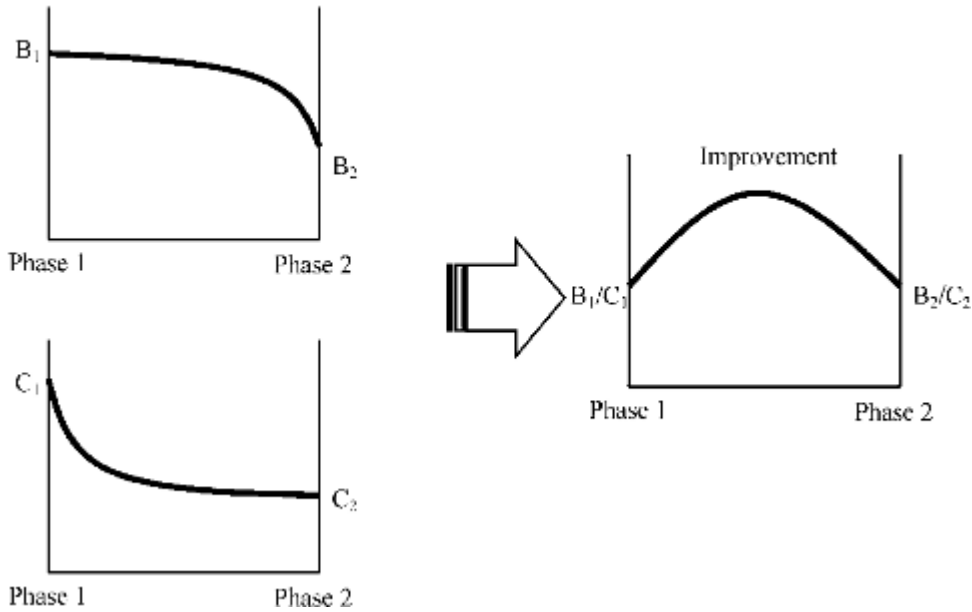


Figure 1.3.1: Graphic scheme of composite properties [21]

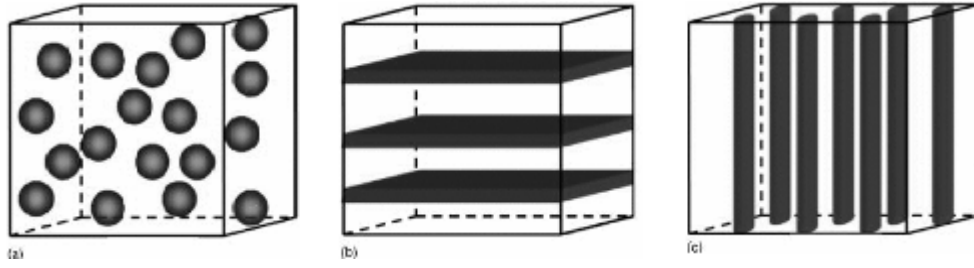


Figure 1.3.2: Schematic illustrations of three composites with different connectivity schemes: a) 0-3 particulate composite, b) 2-2 laminate composite, c) 1-3 fiber/rod composite [22]

The fact that the combination of piezoelectricity and magnetostriction results in a large magnetoelectric response to a magnetic field at room temperature makes magnetoelectric composites very intriguing for technical application and enhanced intensive research for suitable material compositions.

1.3.1 Types of ME Composites

Over the years three different kinds of ME composites have been established from a microstructural point of view (also see Fig.:1.3.2).

- A 0-3 type particulate composite, which is generally a magnetoelastic material embedded in a piezoelectric matrix
- A 2-2 laminated structure, consisting of multilayered magnetostrictive and piezoelectric materials
- A 1-3 fiber composite, with fibers of one phase embedded in the other phase, e.g. self assembled, monolayer nanostructures

All of those different types of composites offer a variation of advantages and disadvantages. Particulate composites (0-3) are in most cases very easy to produce, e.g. through standard ceramic processes. However, the use of ferrites in those ceramic composites often deteriorates the insulation of the final material as a result of the conductive or semi-conductive behavior of most ferrites. Leakage problems restrict the polarization process and thus lower the possible ME output. To overcome this problem a high dispersion of

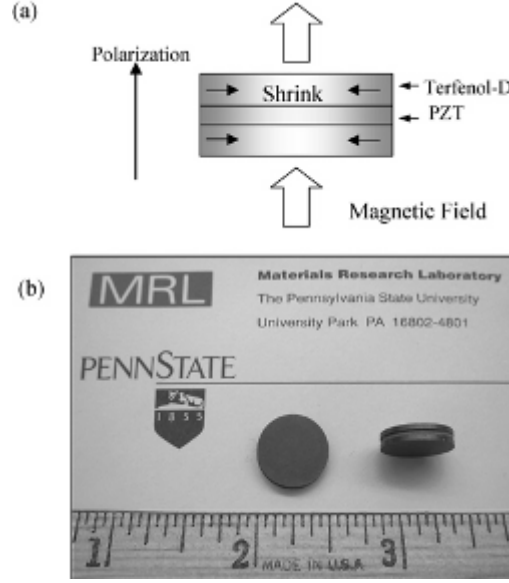


Figure 1.3.3: ME laminate composite using Terfenol-D and PZT discs. a) schematic structure, b) photograph of the composite [21]

ferrite particles in a piezoelectric matrix is desired. Several approaches were taken to achieve such a structure, e.g. core-shell type composites [23], but until now materials with a ferrite core in a piezoelectric shell have not been ideally realized due to difficulties in the very complex chemical preparation.

Compared to the particulate composite ceramics, 2-2 laminate composites with alternating ferrite and piezoelectric layers, show a higher ME effect due to elimination of the leakage problem. Intriguing ME voltage coefficients were presented by Ryu et al. [21], who combined the highly magnetostrictive alloy Terfenol-D with PZT by bonding discs together by means of an epoxy-based adhesive and ME voltage coefficients were $\sim 5 \text{ V}/(\text{cm} \cdot \text{Oe})$ at a bias field of $H_{\text{dc}} = 4000 \text{ Oe}$ and $H_{\text{ac}} = 1 \text{ Oe}$ at 1 kHz .

Following this publication many others synthesized laminated composites of highly magnetostrictive alloys and mostly PZT or piezoelectric single crystals. Dong et al. [24] reported a giant magnetoelectric voltage coefficient by combining a 1D phase connected piezoelectric PZT-fiber layer laminated between two two-dimension (2D) phase connected high-permeability magnetostrictive FeBSiC alloy (Metglas, amorphous alloy ribbon, produced by

rapid solidification) foils, forming a magnetoelectric laminate with a (2-1) phase connectivity, reaching a ME voltage coefficient of $\alpha=22$ V/(cm*Oe) at $H_{dc}=4$ Oe and $H_{ac}=1$ Oe at 1 kHz.

However bonding by means of a strong epoxy adhesive leads to losses in the translation of strain since even thin layers of adhesive absorb the strain partly. For the very temperature sensitive magnetic alloys high temperature processing is not possible. For ceramic oxides co-firing processes proved quite successful [25]. Similarly to the 0-3 type particulate composites high temperature sintering is still a challenge. Occasionally high temperature triggered interdiffusion between magnetic and ferroelectric materials and deteriorated interfacial coupling. Additionally thermal expansion mismatch between two phases can lead to pores or cracks during cooling and consequently high ME response in cofired laminated composites is not easy to achieve. In multilayered structures ME signal loss occurs due to non sufficient conductivity of the ferrite phase. The losses can be reduced by introduction of internal electrodes (e.g. Ag, Ni) between ferroelectric and magnetic layers.

1.3.2 Nanostructured Composite Thin Films

Developement of modern proccessing techniques like pulsed laser deposition (PLD), molecular beam epitaxial, and sputtering, and chemical processing, such as sol-gel and spin-coating initiated research and production of nanostructured ME composite films in recent years [26, 27, 28]. Compared to bulk ME composites nanostructured films offer additional degrees of freedom, such as lattice strain or interlayer interaction to modify ME behavior. The coupling interaction between magnetostrictive and piezoelectric phases is still due to elastic interaction but enhanced interfacial bonding in nanostructured composites strongly affects the ME output.

Similarly to bulk ceramic composites there are also three types of nanocomposite thin films [22]:

- 0-3 type structures with magnetic spinel nanoparticles embedded in ferroelectric films. Wan et al. synthesized a PZT-CFO composite using a sol-gel process and spincoating technique. The films show good

ME performance of $\sim 300 \text{ mV}/(\text{cm} \cdot \text{Oe})$ and strong dependence on magnetic field frequency [29]. This type of structure however has not been reported very often compared to the following.

- 1-3 type heterostructures (vertical nanostructures) were the first ME nanocomposites reported by Zheng et al. [27]. CoFe_2O_4 nanopillars were embedded into a matrix of BaTiO_3 by means of pulsed laser deposition. Although design and control of such heterostructures is a demanding challenge these 1-3 type nanofilms have gained the substantial attention in recent years. ME coupling has been demonstrated through switching of the magnetization through reversal of electric polarization [30]. A reduced clamping effect by the substrate and a more efficient strain coupling resulting from a larger interfacial surface area provided by the vertical architecture could explain such behavior. However a direct measurement of the ME coefficient has not yet been reported due to leakage problems resulting from low resistance of the magnetic pillars in the ferroelectric matrix.
- 2-2 type heterostructures (horizontal nanostructures) consisting of alternate layers of ferroelectric and magnetic oxide. These structures are easier to fabricate and leakage problems do not occur. However the ME effect is rather weak compared to other composite types due to large in-plane constraints from substrates. Several 2-2 type combinations of ferroelectric perovskites (BTO, PZT) and magnetic oxides (CFO, NFO) have been grown via PLD or sol-gel spincoating processes and summarized elsewhere [22].

1.4 Applications

The possibility to influence electric polarization through a magnetic field or magnetization through an electric field makes magnetoelectric materials extremely interesting for a wide range of applications such as sensors, transducers, filters, oscillators, phase shifters, memory devices, microwave devices and so on.

Especially bulk composites exhibiting the ME effect at room temperature as well as single phased BiFeO_3 have drawn great attention for implementation into new technologies.

1. **Magnetic Sensors:** Exposing a magnetoelectric material to a magnetic field, the magnetic phase strains and produces a proportional charge in the piezoelectric phase. Therefore highly sensitive magnetic field sensors can be produced using materials with high ME coefficients. Dong et al. [31] reported a novel push-pull layered composite of Terfenol-D and $\text{Pb}(\text{Mg}_{1/3}\text{Nb}_{2/3})\text{O}_3$ which showed high sensitivity to ac-fields from 10^{-11} T to 10^{-3} T. Operated at resonance frequency of $f=77,5$ kHz the sensitivity even reached $1,2 \times 10^{-12}$ T. Israel et al. found ME behavior in industrially manufactured multilayered capacitors (MLCs). Cost-saving replacement of Ag and Pd in electrodes with Ni in MLCs with BaTiO_3 as dielectric enabled direct ME effect in mass producible MLCs at a unit price of 1 Cent [32]. The maximum ME output $dV/dH=7$ mV/(cm*Oe) which is not large but given the cheap production cost, room temperature function without additional electric power make those MLCs very interesting for magnetic field sensors, transducers or energy harvesters.

2. **Energy Harvesting:** The desire for wireless charging of electronic devices by converting ambient energy into electric energy has become a huge field of present research [33, 34]. An ME energy harvester typically consists of one or multiple cantilever beams, a magnetic circuit and a ME composite, see Fig.1.4.1a). The ME transducer, a ferroelectric sandwiched between two magnetostrictive layers is placed on the tip of the cantilever which vibrates within the magnetic circuit shown in Fig. 1.4.1b), e.g. NdFeB permanent magnets.

Vibration of the cantilever causes relative motion between the ME transducer and the magnetic circuit and through alternating magnetic field the magnetostrictive phase will generate stress which is transferred to the ferroelectric and consequently electric charges are produced. These transducers typically work best at their respective resonance fre-

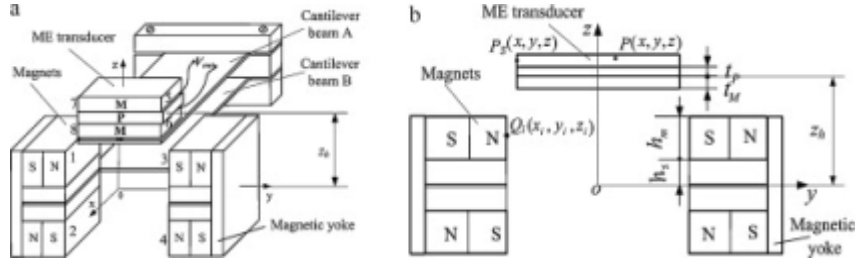


Figure 1.4.1: Schematic diagram of a ME energy harvester a) and the ME transducer in the permanent magnetic field b) [33]

quency, consequently for technical application a broad frequency band and low frequencies are desired and subject of current research.

3. **Transformers:** Dong et al. recently designed and prototyped resonance type laminated composites with strong ME coupling and a large voltage gain effect [35, 36]. Long type ME laminates consisting of Terfenol-D and PZT layers showed a large gain of the input ac-voltage at the laminate's resonance frequency due to strong magnetoelectric coupling. The large voltage gain under resonant drive offers great potential for high-voltage miniature transformer applications.

Fig.1.4.2 shows the voltage gain V_{out} / V_{in} as a function of the drive frequency for a ME transformer. In addition to the frequency dependence the ME output also strongly depended on the DC-bias field because of the field dependence of the piezomagnetic coefficient of Terfenol-D.

4. **Microwave Devices:** Microwave signal processing devices such as resonators, phase shifters or filters are an important part of modern technology. ME ceramic composites represent a promising new approach for a new class of fast electric field tunable, low power microwave devices compared to the state-of-the art magnetic tuning, which is slower and more energy consuming. Application of an electric field E to a piezoelectric transducer results in a mechanical strain coupled to the ferrite and consequently leads to a shift of the resonance field [37].

Fetisov et. al presented a device concept for a magnetoelectric microwave resonator that is tunable by an electric field and working based

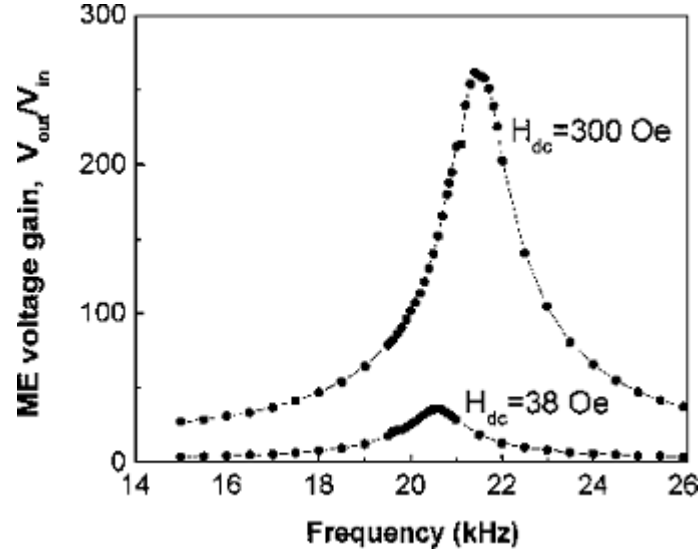


Figure 1.4.2: Voltage gain of ME transformer, consisting of Terfenol-D and PZT layers, as a function of the drive frequency. Under resonant drive a voltage gain factor of ~ 270 is achieved, magnetic bias field influences the resonance frequency as well as the gain factor [35]

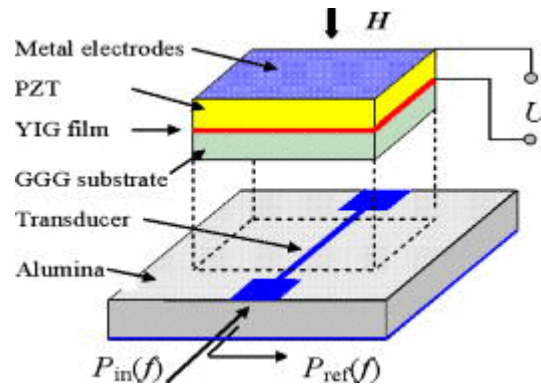


Figure 1.4.3: Diagram showing a microstripline resonator with a bilayer of lead zirconate titanate (PZT) bonded to (111) yttrium iron garnet (YIG) film on gadolinium gallium garnet (GGG) substrate [38]

on the principle mentioned above. Through the application of the electric field a shift of the FMR (ferromagnetic resonance) due to the strain in the ferrite was observed. Since YIG resonators form the basis for bandpass and bandstop filters YIG-PZT resonators would allow faster and energy efficient electric field control of such devices [38].

5. **Memory Devices:** The possibility of controlling the magnetization via an electric field or electric polarization via a magnetic field makes magnetoelectric materials interesting for the development of novel memory devices. Both ferroelectrics and magnetic materials are up to now in use for binary memory storage in FeRAMs (ferroelectric random access memory) and MRAMs (magnetic random access memory). FeRAMs offer fast access speeds and high densities but require destructive read and reset operations. MRAMs however cannot achieve comparable access speeds and are more energy consuming, however suffer no limitations concerning their endurance.

The combination of the best properties of both types of memories could be achieved through magnetoelectrics allowing fast low power electric writing operations and non-destructive magnetic data reading [39]. In those novel MERAMs magnetoelectric coupling enables to control the magnetization of the ferromagnet via the coupling interface between the ferromagnet and the multiferroic so that ultimately the magnetization can be switched by the electric polarization of the multiferroic.

In BiFeO_3 as mentioned in Sec. 1.2.1 the coupling of antiferromagnetic and ferroelectric order parameters has been observed recently [19]. Chu et. al were the first to report magnetoelectric manipulation of magnetization at room temperature. Small micrometer sized CoFe elements were deposited on BFO films and subsequently the magnetic domain structure of the CoFe exhibits systematic coupling with the antiferromagnetic spins in BFO. Application of an in-plane electric field modifies the domain structure of the CoFe particles by rotating the magnetization 90° . A reversal of the effect occurs by applying a field with opposite polarization [40].

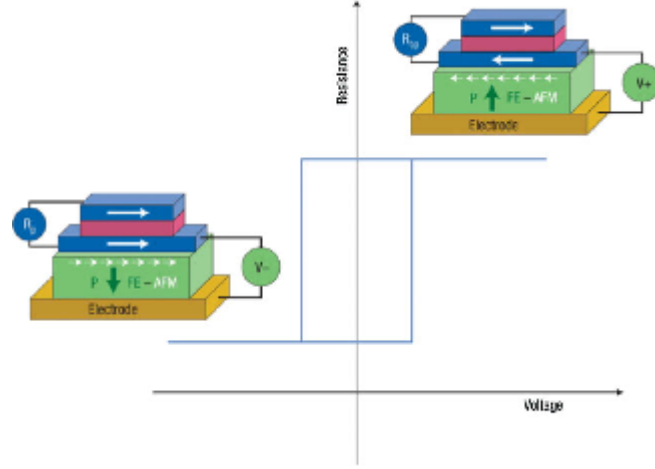


Figure 1.4.4: Sketch of a possible MERAM element. [41]

These experiments present a huge step towards novel magnetoelectric memory devices although many issues remain unresolved, such as vertical geometry, low write voltages, high frequency operation and nanoscale devices [41].

In Fig. 1.4.4 a schematic diagram of a MERAM element is presented. The binary information is stored by the magnetization direction of the bottom ferromagnetic layer (blue), read by the resistance of the magnetic trilayer (R_p when the magnetizations of the two ferromagnetic layers are parallel), and written by applying a voltage across the multiferroic ferroelectric–antiferromagnetic layer (FE-AFM; green). Sufficient coupling presumed reversing the polarization in the multiferroic changes the resistance of the magnetic trilayer from parallel to antiparallel resulting in a hysteretic dependence of the device resistance with the applied voltage.

1.5 Objectives Of This Work

The main purpose of this work is to implement a new measurement technique for magnetoelectric characterization as well as to explore new synthesis routes for magnetoelectric bulk composites. The combination of a Hirst Industrial

Pulsed Field system and a charge amplifier offers a very direct approach for ME measurements. For the novel measurement setup a sample holder for ME composite discs had to be designed and constructed and the charge amplifier had to be implemented and calibrated in an already existing pulse field measurement system.

Parallel new synthesis routes for magnetoelectric composites of magnetostrictive CoFe_2O_4 and piezoelectric BaTiO_3 or $\text{Pb}(\text{ZrTi})\text{O}_3$ were explored. Following the establishment of a sol-gel synthesis route all prepared samples were investigated by microstructural, magnetic, magnetostrictive and magnetoelectric measurements.

Variation of production parameters such as stoichiometry, sintering temperature, pressing and polarization conditions on the physical properties of the composite powders were investigated in several experiments in order to find an optimal production routine for maximum magnetoelectric output and increase the understanding of influencing factors on the ME coefficient.

Chapter 2

Measurement Technique

2.1 Methods For ME Characterization

Although the research in magnetoelectric effect experienced a huge renaissance over the last decade, there still is no general method for determining the magnetoelectric performance of respective materials. Therefore a comparison of experimental results is difficult and a well established, reliable measuring technique is desperately needed.

Meanwhile a broad variety of different measuring methods has been published. A few years ago a static or quasi static methods were introduced. Both use a high impedance electrometer and a DC magnetic field. The ME signal is defined as a function of the magnetic field in the static method [42] and as a function of time by varying the magnetic field linearly in the quasi static method [43].

A very common way of determining the magnetoelectric effect is a dynamic approach where a AC magnetic field, produced by a Helmholtz coil, is superimposed to a parallel DC bias field H provided by an electromagnet. The sample is placed in the magnetic field and the resulting AC voltage caused by the electromagnetic effect is measured by using a Lock-In amplifier [44]. The resulting ME coefficient is

$$\frac{dE}{dH} = \frac{V_{out}}{h_0 d}$$

where d is the effective thickness of the sample, V_{out} is the output voltage and h_0 is the amplitude of the AC field.

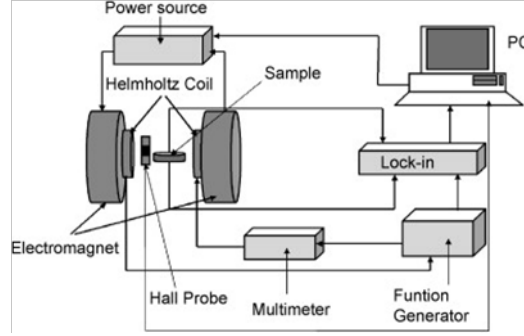


Figure 2.1.1: Scheme of experiment setup for the dynamic method. An AC magnetic field, produced by the Helmholtz Coil is superimposed to a DC bias field from electromagnets. AC-voltage caused by ME interaction in the sample is measured using a Lock-In amplifier.[44]

By using a charge amplifier instead of a Lock-In device a more direct way of measuring the magnetoelectric effect can be provided [21, 45]. Here also a small magnetic AC field is superimposed to a DC bias field and the magnetoelectric charge generated in response to the AC field is directly measured by means of a charge amplifier, converting the charge signal into a proportional output voltage which is subsequently read out with an oscilloscope.

The dynamic method however cannot provide a direct measurement of the ME response to a magnetic field, only the variation of it in response to the AC field. As pointed out in [44] there are several other disadvantages such as discharging processes due to the sample's resistance at low and the capacitance at high frequencies.

Using a pulsed magnetic field eliminates some of the mentioned problems. The voltage across the sample in response to a magnetic pulse of 4-50 ms duration is amplified and filtered with a high impedance preamplifier operated in differential mode to avoid induction voltages in the set-up and further processed using a measurement card [46, 47].

Fetisov and others also used a pulsed field technique to study frequency dependence of NFO-PZT laminated composites by varying the duration of

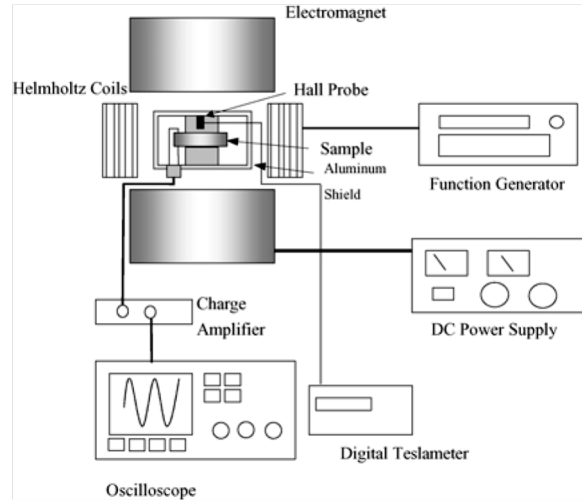


Figure 2.1.2: Dynamic method using a charge amplifier. Electric charges in the ME sample, caused by AC field modulation of the Helmholtz Coils, are collected by the charge amplifier, converted into a voltage signal and processed by means of an oscilloscope [21]

the magnetic pulse [48]. ME measurements through piezoelectric coupling, were a standard, quasi-static piezoelectric coefficient measurement system is combined with a magnetic DC bias field and a small AC field are also possible [49], as well as the use of a magnetic cantilever to generate AC fields up to 10^3 Oe to induce ME voltage response in epitaxial nanocomposite films of BeFeO_3 - CoFe_2O_4 [50].

By using the advantages of modern SQUID magnetometry Borisov and others went away from the more convenient measurement of polarization induced by magnetization and observed the ME effect by applying an electrical field through thin copper wires directly on the surface of the Cr_2O_3 sample [51].

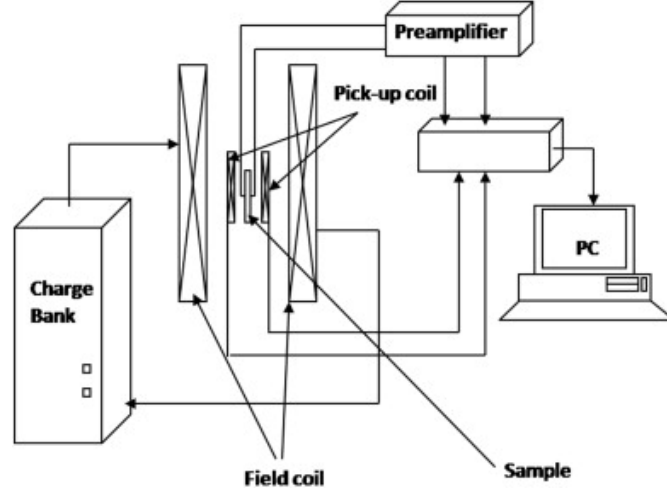


Figure 2.1.3: Scheme of the pulse field method for ME characterization. The voltage across the sample in response to a magnetic pulse is amplified and filtered with a high impedance preamplifier operated in differential mode and further processed using a measurement card [46]

2.2 The Pulse Field Method Utilizing a Charge Amplifier

As stated in section 2.1 the pulse field method offers several advantages compared to the dynamic method: frequency dependance and discharging processes as well as a decreasing modulation field at high frequencies among them. Therefore our group developed a pulse field method using a Hirst Industrial System pulse field arrangement. Giap [46] measured the ME response to the magnetic pulse through the induced voltage across the sample by means of a voltage amplifier operated in differential mode. However his self-designed sample holder was only applicable for samples with a narrow range of thickness.

Our first goal was the design and construction of a new sample holder in order to perform magnetoelectric measurements regardless of the sample's thickness, with the magnetic field perpendicular to the sample surface. For stability reasons and non-magnetic behavior poly-vinyl-carbonate (PVC) was chosen as basic material. Three electric pins with an internal spring fix the

sample disc on one side, while on the other side a copper-plate on a small PVC disc presses the sample against the pins by means of a PVC screw, as seen in Fig.2.2.1. This allows fixing and simultaneously generates the necessary electric contact to the charge amplifier for a sample thickness ranging from 0.5 mm to a few cm if necessary. Since we are working with a charge amplifier, a specially screened low noise cable connects the electric contacts to the measurement system. Using a conventional cable would induce small noise charges due to cable movement and thus disturb the measurement.

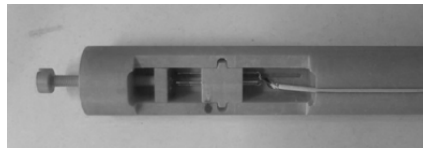


Figure 2.2.1: Top of the PVC sample holder where the sample is fixed between a copper-plate and three electric pins. The distance between pins and plate can be adjusted by the PVC screw on the left.

2.2.1 The Charge Amplifier (Kistler 5001)

Using a charge amplifier instead of a voltage amplifier offers the most direct approach for ME measurement since piezoelectric materials exhibit an electric charge when experiencing mechanical stress. Additionally the non-infinite input impedance, as well as the high resistance of the electrically insulating sample, can cause measurement errors.

By means of the charge amplifier the generated charge is converted into a proportional output voltage, which is used as an input variable for our analysis system. A charge amplifier basically consists of an inverting voltage amplifier with a high open loop gain and a capacitive negative feedback. The resulting output voltage just depends on charge input and on the range capacitance $U=Q/C$.

The charge amplifier acts as an integrator compensating the generated charge with one of equal magnitude and an opposite polarity of the range capacitor. The voltage across the capacitor is proportional to the incoming charge and allows the mentioned conversion of a charge into a usable



Figure 2.2.2: Kistler Charge Amplifier 5001

voltage. The selection of the range capacitor also defines the magnitude of amplification.

The output voltage of the charge amplifier undergoes further amplification in an operative amplifier with adjustable negative feedback. The adjustment is done by means of a potentiometer allowing the device to adapt the output voltage to a certain calibration constant of an upstream measurement device. In our case this is of course not necessary, we used the built-in potentiometer to exactly calibrate the charge amplifier. Two high-ohm resistances and a short circuit relay are connected in parallel to the range capacitor. Short circuiting the capacitance completely discharges the amplifier and sets the output voltage to zero. The resistances discharge the capacitance slowly with a time constant $T=RC$ preventing drifting but making quasi-static measurements impossible.

2.2.2 Operating the Charge Amplifier

In order to use the device the “operate-reset-remote”- switch must be set to operate. In the “reset-mode” the range capacitance is short circuited and the output voltage always zero. For our measurements in the pulsed field it proved useful to switch to the operate mode just seconds before the pulse

and stay in reset mode the rest of the time. The “short-long-medium” switch defines the time-constant. For pulse-field measurements the setting short is evident whereas for calibration the switch is set to “long”. Short or medium time constant simply means that a high resistance is connected in parallel to the range capacitance thus allowing a slow discharge and consequently preventing charges from eddy currents and drifting.

The range capacitance set to 10^3 and the potentiometer to ~ 10 (which means 1) the amplifying factor becomes 1. We used 3 different range settings of 10^3 , 5×10^2 and 10^2 resulting in amplifying factors 1, 2 and 10.

2.2.3 Calibration of the Charge Amplifier

The calibration of the charge amplifier can be done by means of an integrated calibration capacitor with a 1000 pF capacitance. By means of this capacitor an input voltage generates a charge which undergoes amplification and thus generates an output voltage. With each mV voltage a charge of 1 pC is generated. By means of the negative feedback potentiometer the output voltage can be adjusted to the input voltage.

In our case we aimed for equality of input- and output voltage with a range capacitance of 1000 pF corresponding to calibration capacitance. A Siemens “DC-Konstanter” device was used as the source of DC voltage. An Amprobe 38XR-A multimeter is connected in parallel to check the input voltage. The output voltage is measured by a Keithly multimeter. The input is set to 4.007 V and by setting the potentiometer to 10.2 the output voltage is adjusted to the same value with an amplifier setting of 1.

Afterwards the adjustment is checked with different input voltages and amplifier settings whereas it makes no difference whether the amplifier is disconnected between measurements or the settings are changed in operating mode. In order to prevent possible drift and thus offset voltage we switched off the amplifier between the adjustments to completely discharge the device.

2.3 Discussion of Units of the ME effect

Although the magnetoelectric effect has been studied intensely over the past decades there is still no generally established method for determining the magnetoelectric performance of respective materials. As a consequence a comparison of the magnetoelectric performance of a certain compound is difficult. Discussions concerning a generally accepted system of units for the magnetoelectric coefficient are even more controversial.

Looking at the function of the free energy of a material $g(\mathbf{E}, \mathbf{H})$ ([VAs/m³] = [J/m³]) at zero mechanical stress and developed in a limited Maclaurin series (Taylor series at $\mathbf{x}_0 = 0$) of the two variables \mathbf{E} and \mathbf{H} . [43]

$$g(E, H) = g_0 - P_i^s E_i - M_i^s H_i - \frac{1}{2} \varepsilon_0 \varepsilon_{ik} E_i E_k - \frac{1}{2} \mu_0 \mu_{ik} H_i H_k - \alpha_{ik} E_i H_k - \frac{1}{2} \beta_{ijk} E_i H_j H_k - \frac{1}{2} \gamma_{ijk} H_i E_j E_k - \dots, \quad (2.3.1)$$

where ε_0 and μ_0 are the free space permittivity and free space permeability. Spontaneous polarization and magnetization are denoted P^s and J^s respectively. The tensor of the linear electric effect is referred to as α whereas β and γ are tensors of the bilinear ME effects.

Differentiation of g in respect to \mathbf{E} and \mathbf{H} gives us the total polarization \mathbf{P}

$$P_i(\vec{E}, \vec{H}) = -\frac{\delta g}{\delta E_i} = P_i^s + \varepsilon_0 \varepsilon_{ik} E_k + \alpha_{ik} H_k + \frac{1}{2} \beta_{ijk} H_i H_k + \gamma_{jki} H_j E_k + \dots$$

and magnetization \mathbf{M}

$$M_i(E, H) = -\frac{\delta g}{\delta H_i} = M_i^s + \mu_0 \mu_{ik} H_k + \alpha_{ji} E_j + \beta_{jki} E_i H_j + \frac{1}{2} \gamma_{ijk} E_j E_k + \dots$$

where P and M are spontaneous polarization and magnetization.

For the linear magnetoelectric effect with $E=0$ (ME_H - effect) we get

$$P_i = \alpha_{ik} H_k$$

With P [As/m²] and H [A/m] the second rank tensor α is expressed in [s/m] in the SI-unit-system respectively. In the Gaussian unit system α is dimensionless. In order to determine α we apply a magnetic field δH and measure the electric response δP or δE . An important parameter is the magnetoelectric voltage coefficient $\alpha_E = \delta E / \delta H$. It relates to α through

$$\alpha = \varepsilon_0 \varepsilon_r \alpha_E$$

with ε_r as the relative permittivity of the material. In SI-units α_E is expressed in [V/A] but over the past decades a mixed system of units has been generally used to express α_E in V cm⁻¹Oe⁻¹.

Some groups have used the opposite approach and determined the magnetic response to a change of the electric surrounding. In that case we obtain a $\alpha_H = \delta H / \delta E$.

However especially in novel epitaxial nanocomposite films the ME effect can be detected but not quantitatively determined due to leakage currents on the coupling surface between the ferroelectric and the magnetic phase, which will be discussed later. By means of modern microscopy techniques like MFM (magnetic force microscopy) or PFM (piezoresponse force microscopy) magnetoelectrically induced switching of polarization or magnetization are observed optically [30, 19, 40], see Fig 2.3.1.

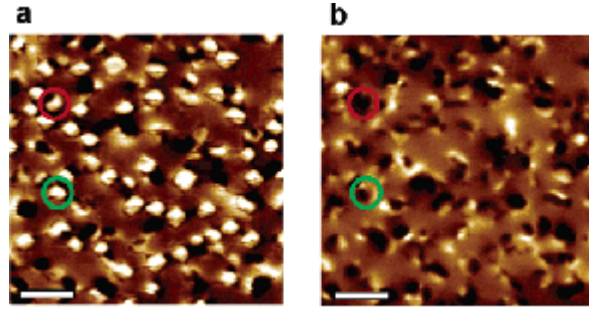


Figure 2.3.1: Changes in the magnetic configuration of a $(\text{BiFeO}_3)_{0.65}-(\text{CoFe}_2\text{O}_4)_{0.35}$ film upon electrical poling. Magnetic force microscopy (MFM) image taken (a) after magnetization in an upward oriented 20 kOe perpendicular field, and (b) after electrical poling at +12 V [30]

Chapter 3

Experimental Procedures

3.1 Chemical Synthesis

3.1.1 Synthesis of CoFe_2O_4 via a nitrate-citrate gel combustion route

Various synthesis routes for CoFe_2O_4 are well known. Most common are standard ceramic ball milling, glycine-nitrate auto-combustion synthesis [52] or certain sol-gel processes [53]. Later mentioned are very popular hence they allow the production of single-phased nanopowders with a homogeneous microstructure at relatively low temperatures and shorter reaction times compared to ceramic ball milling. For reasons of reproducibility, magnetostrictive performance and cost, a modified nitrate-citrate gel combustion method was chosen for this work.

Therefore stoichiometric amounts of $\text{Fe}(\text{NO}_3)_3 \cdot 9\text{H}_2\text{O}$ (Aldrich, 98%), $\text{Co}(\text{NO}_3)_2 \cdot 6\text{H}_2\text{O}$ (Merck, 98%) and $\text{C}_6\text{H}_8\text{O}_7$ (Aldrich, 99%) were dissolved in deionized water and afterwards mixed in a 800ml beaker. The citric acid serves two purposes in this reaction. First of all it allows the complexation of the metal ions and second it works as a fuel for the combustion reaction. The nitrate ions of the metal precursors however constitute a redox environment thus acting as oxidant.

The molar ratio of nitrates and citrates was 1:1 respectively. The mixture

of the red cobalt-nitrate solution and the yellow iron-nitrate solution together with the non-coloured citric acid yields a dark brown solution. In order to adjust the pH-value to 6-7 liquid ammonia (25%, Aldrich) is added dropwise under constant stirring (magnetic stirrer) by means of a Pasteur-pipette. The pH value of the reaction solution is monitored with a pH-meter, see Fig. 3.1.5. When the desired pH-value is reached the solution is allowed to evaporate maintaining a temperature of 80-90°C. Depending on the amount of water used of dissolving of the precursors this takes about 1.5 to 2 hours.

Evaporation leads increased viscosity and a dark brown, honey like gel starts to form. Further increase of the temperature of the heating plate to 200°C allows the gel to slowly combust into a voluminous dark grey ash. The reaction takes about 10-20 seconds starting at the hottest zones of the beaker and comes with emission of large amounts of gas and smoke, additionally small sparks occur. Below the calculations for the reaction are presented: The molar mass of CoFe_2O_4 is 234.62 g/mol. For the production of 0.025 mol of CoFe_2O_4 we need:

$$0,025 \text{ mol Co(NO}_3)_2 \cdot 6\text{H}_2\text{O (291,03 g/mol)}$$

$$0,05 \text{ mol Fe(NO}_3)_3 \cdot 9\text{H}_2\text{O (403,99 g/mol)}$$

Therefore we have 0.075 mol of metal nitrates which means we need 0.075 mol of $\text{C}_6\text{H}_8\text{O}_7$ (192,12 g/mol) to get the desired 1:1 ratio of nitrate/citrate.

3.1.2 Synthesis of BaTiO_3 - CoFe_2O_4 Composites

The synthesis of core-shell type magnetoelectric composites with magnetostriuctive CoFe_2O_4 as a core surrounded by a piezoelectric shell of BaTiO_3 has been done successfully by various groups e.g. [54][23][55]. In principle BaTiO_3 is synthesized via a sol-gel route with CoFe_2O_4 particles present. The gel surrounds the ferrite-particles thus forming a core-shell structure. The ratio of $\text{BaTiO}_3/\text{CoFe}_2\text{O}_4$ was 1:1 in mass.

For the reaction a stoichiometric amount of $\text{Ba}(\text{CH}_3\text{COO})_2$ is dissolved in 0.5M acetic acid. The ferrite powder is introduced into the viscous Ti(IV)

butoxide followed by the acetate solution. Immediately a thin white skin develops on the surface due to hydrolysis of the butoxide. The reagent is put into an ultrasound bath at a temperature of 75°C and the water slowly evaporates. During the evaporation process it is useful to mechanically stir the solution with a glass stick every 5-10 minutes. Alternatively the reagent was allowed to evaporate on a heating plate stirred magnetically or by means of a rotary evaporator. The resulting grey powder is dried in air over night, presintered at 700°C for 2 hours (heating rate 3.9°C/min), mechanically grinded by hand, pressed into pellets axially (6t/cm²) and finally sintered at 1000°C (heating rate 2.3°C/min) for 12 hours.

For 2g of composite material (1:1 ratio of the constituents) we need 1g CoFe₂O₄(=4.26mmol) and 1g BaTiO₃(=4.29mmol)

$$4.29 \text{ mmol Ba(CH}_3\text{COO)}_2(255.42 \text{ g/mol})$$

$$4.29 \text{ mmol Ti(IV) butoxide (340.36 g/mol)}$$

$$8.58 \text{ mmol } 0.5\text{M CH}_3\text{COOH} = 17.15 \text{ g}^1$$

Acetic acid (96% Aldrich) has to be diluted to obtain a concentration of 0.5M. ²

3.1.2.1 Problems

Although XRD-analysis confirmed the desired composite structure of CoFe₂O₄ and cubic BaTiO₃ with small impurities of BaFe₁₂O₁₉ the magnetoelectric performance of previously reported materials [23] couldn't be matched. From a chemical point of view the synthesis of BaTiO₃ looks like a precipitation process instead of gelation leaving the evolution of a core-shell type structure questionable.

Additionally the polarization process proved to be problematic. Even at small electric field strengths leak currents occurred at temperatures above 120°C, implementing that the composite material was not a proper electrical

¹ $\frac{8.58 \text{ mmol}}{0.5 \text{ mol/l}} = 0.01715 \text{ l} \Rightarrow 0.01715 \times 1000 \text{ g/l} = 17.15 \text{ g}$

² 96% equals 16.79M \Rightarrow 0.03l in 1l H₂O or 1.58g in 50ml H₂O

insulator. The reason for this unfortunate behavior could lie within the structural complexity of BaTiO_3 where even small variations and impurities in the lattice have a large impact on the ferroelectric behavior.

3.1.3 Synthesis of CoFe_2O_4 -PZT composites by nitrate-citrate combustion

Because of the unfortunate problems with the Bariumtitanate composites we replaced BaTiO_3 , with PZT as piezoelectric constituent of the composite. PZT is the acronym for $\text{Pb}(\text{ZrTi})\text{O}_3$. Like BaTiO_3 PZT is a perovskite and usually a molar ratio between Zirconium and Titanium of 52:48 is common for piezoelectric behavior. For our purposes commercially available PZT was bought from “Noliac”. The material labeled NCE55 was chosen for its high sensitivity featuring high permittivity, large coupling factor and piezoelectric constant and a relatively low Curie temperature [noliac ceramics data sheet, Ver 0901]. The PZT powder is doped with Nb and Ni and is pure and unsintered. The exact stoichiometric composition is not known due to industrial confidentiality.

In-situ gel combustion synthesis of magnetoelectric composites of Cobalt-Ferrite and PZT has been already reported [56, 57]. The process is similar to the synthesis route for CoFe_2O_4 mentioned before in this chapter (Sec. 3.1.1).

After the dissolution and mixing of the precursors $\text{Fe}(\text{NO}_3)_3 \cdot 9\text{H}_2\text{O}$ (Aldrich, 98%), $\text{Co}(\text{NO}_3)_2 \cdot 6\text{H}_2\text{O}$ (Merck, 98%) and $\text{C}_6\text{H}_8\text{O}_7$ (Aldrich, 99%) the pH-value of the reagent is adjusted to 6-7 by means of liquid ammonia (25%, Aldrich). Then the PZT powder was introduced and the solution was stirred thoroughly for 1.5 hours. Under further constant stirring the temperature was raised to 80°C and the water was allowed to evaporate. With continuing evaporation the viscosity of the reagent increases. The magnetic stirrer is removed and the honey like substance evolves into a voluminous brown foam. The temperature of the heating plate is increased further and eventually the foamy substance combusts into a voluminous dark grey ash.

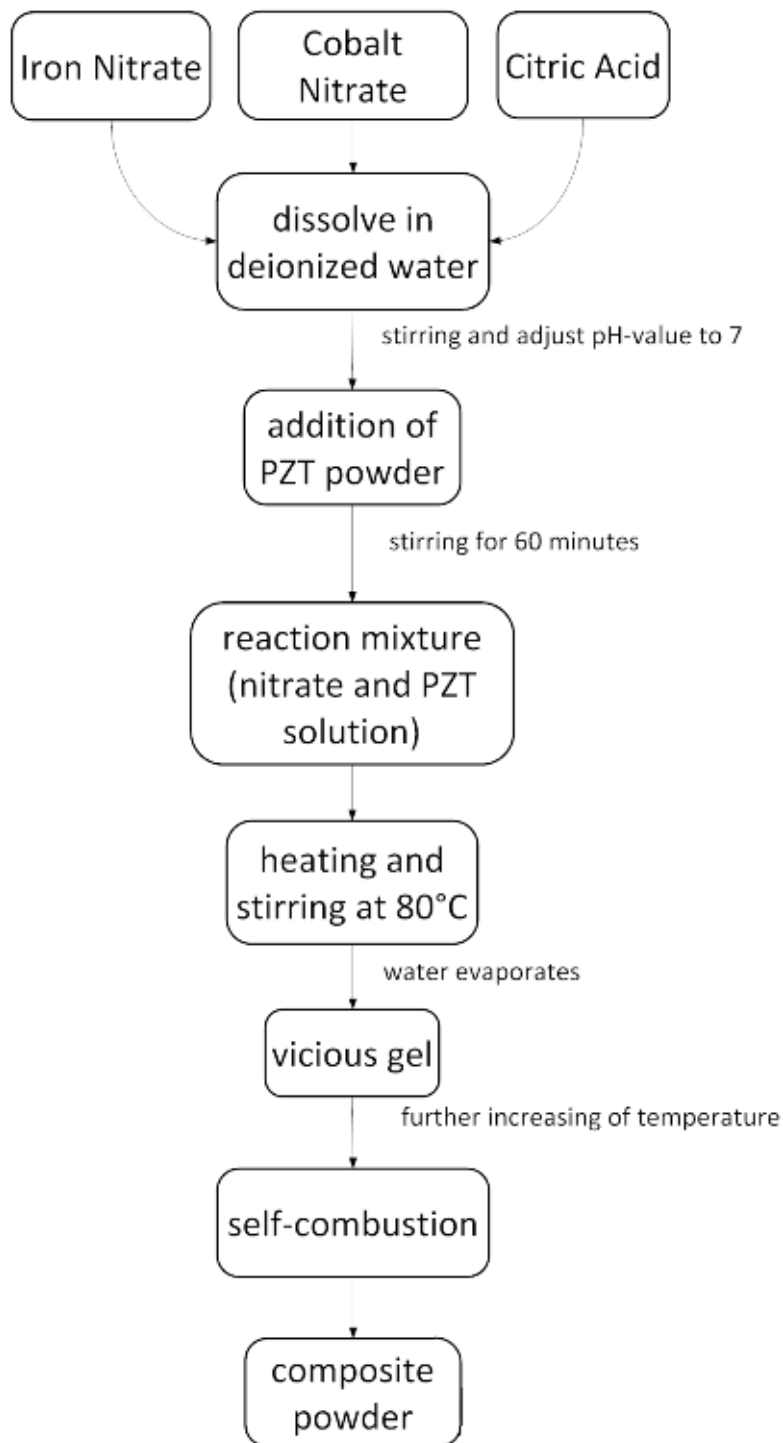


Figure 3.1.1: Flow-Chart of the reaction procedure for CoFe₂O₄-PZT composites



Figure 3.1.2: Precursors for the reaction

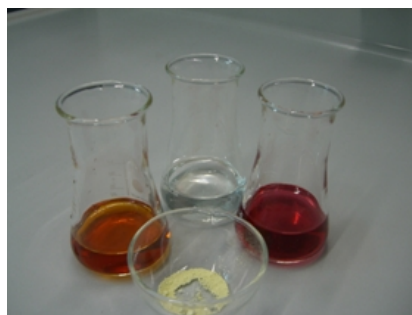


Figure 3.1.3: Precursor solutions

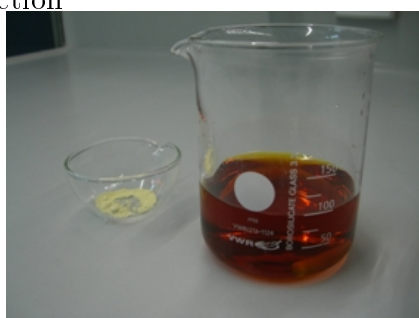


Figure 3.1.4: Reaction solution (all reactants mixed together)



Figure 3.1.5: Adjustment of pH value

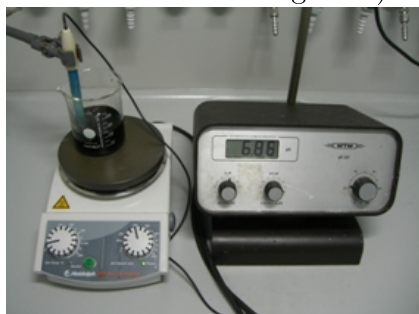


Figure 3.1.6: Solution darkens with rising pH value

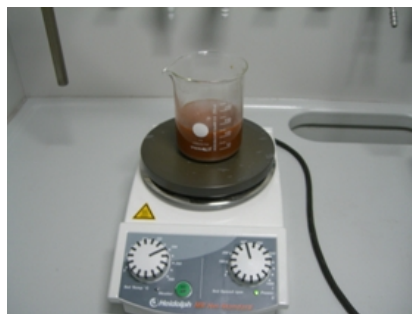


Figure 3.1.7: Adding PZT and heating

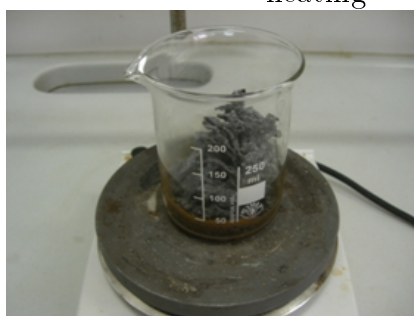


Figure 3.1.8: Composite powder after auto-ignition

3.1.4 Pressing and Sintering

The obtained composite powders were grinded by means of an achate mortar and afterwards pressed. The majority of samples was pressed axially into circular disks (pellets) of 12 mm diameter and a thickness of 0.8-1.2 mm applying a pressure of 6 t/cm²(22.86 MPa). We used 0.4 g of powder for each sample disk. After the desired pressure is reached it is released immediately to avoid the formation of cracks.

The samples CFPZT_14, CFPZT_15 and CFPZT_16 however were pressed isostatically by means of a hydraulic press (P.O. Weber PW 40 uni-axial press with cold-isostatic pressing chamber) at a pressure of 320 MPa. The powder is filled into a silicon matrix which is then covered with a finger of a common lab glove and sealed to avoid contact between sample and fluid (water). It is very important that no air is enclosed to obtain complete homogeneity. The pressure is applied and kept for about one minute and then slowly released over a time period of three minutes. The isostatically pressed pellets have a diameter of 9mm and a thickness of 3-5mm.

After pressing, the pellets were sintered in closed Corundum-crucibles at a temperature of 1000°C for 2 hours in case of the PZT-samples and for 12 hours for the BaTiO₃ samples respectively. The heating rate was 3.25°C/min whereas the cooling rate was 1.67°C/min (naturally cooling down by switching of the furnace). In order to obtain information about the influence of the sintering temperature the samples CFPZT_15 and CFPZT_16 were sintered at 800°C and 600°C.

3.1.5 Thermogravimetric Analysis

To understand the sintering behavior of the composite material, thermogravimetric analysis was carried out at the Institute of Inorganic Chemistry, Technology and Materials at the Slovak University of Technology in Bratislava. TGA-DTA measurements were done on a Perkin Elmer Thermogravimetry/Differential Thermal Analyzer (TG/DTA 6300) from 25-1000°C at heating rate of 10°C/min.

3.1.6 Structural Analysis

A very crucial step in the production of magnetoelectric composites is the structural analysis of the synthesized powders providing substantial information about stoichiometry, micro structure and morphology and their possible influence on magnetic or magnetoelectric performance. X-Ray diffraction (XRD) was used to obtain crystal-structure and chemical purity whereas the surface morphology was determined by Scanning Electron Microscopy (SEM).

The XRD patterns for all the studied samples were recorded by means of an Xpert Philips powder diffractometer (Goniometer Philips PW 3050/60) using $\text{CuK}\alpha_{1,2}$ radiation in a Bragg Brentano geometry, and a X'Celerator detector. The X-ray generator Philips PW 3040/60 worked at a power of 40 kV and 40 mA and the goniometer was equipped with a graphite monochromator. Diffraction patterns were recorded in the angular range 5° to 135° with a scan step size of 0.02° . Collected data were refined using the Rietveld package TOPAS (Bruker AXS Topas V 2.1) based on the fundamental parameter approach, with diffractometer parameters and wavelength settings adjusted using a LaB6 standard [58].

The SEM imaging for this work was performed using a JEOL JSM-6390LV SEM. The maximum resolution power for this particular instrument is 3 nm and possible magnification ranges from 5x to 3×10^5 .

3.1.7 Electric Poling

Magnetoelectric materials exhibit an electric charge when exposed to a magnetic field. Due to the magnetostrictive behavior of the CoFe_2O_4 the piezoelectric components experience a change in dimension resulting in an electric charge in direction of the polarization. However, on a microscopic level all electric moments of the piezoelectric phase are distributed statistically leaving the resulting charge zero by the principle of superposition. This fact can be overcome by exposing the sample to a sufficiently high electric field enabling an ordering of the electric moments.

The sintered samples were slightly grinded with grinding paper and coated

with silver paste for electrical contact. Circular copper-plates (3.5 cm diameter, 1.2 mm thickness) were used as capacitance. The discs were put in between the plates, sealed with Teflon foil and clamped to the high voltage DC power provider (Heizinger HCNs 3500-100) allowing a maximum voltage of 3kV. The capacitance system was then put into a silicon oil bath and subsequently heated to 140-170°C in order to exceed the ferroelectric-dielectric transition temperature for either BaTiO₃ or PZT. As soon as the desired temperature was reached the electric field of 3-4 kV/cm was applied (sample thickness \sim 1 mm means 300V voltage). The oil was kept at the desired temperature for 20 minutes and then allowed to cool down naturally with the electric field still on. The process takes 1.5-2 hours. The oily sample is cleaned with wipes and ethanol and then ready for measurement.

3.1.7.1 Problems

The process of electric poling is not only very important for the magnetoelectric performance it is also caused some inconvenience during the experimental phase. Initially we used an epoxy based silver paste to directly attach copper wires to the sample discs, which turned out to be not only mechanically difficult but also ineffective due to the inhomogeneity of thickness of the electrodes. The copper electrodes proved to be more effective, however it is very important to use blanked plates instead of cut ones, since cutting causes sharp edges where sparks may occur when high voltage is applied.

Two different kinds of silver paste were tried and only one (62900341 Ag Leitsilber 204, purchased at Conrad Electronics) performed sufficiently. The other one (RS-Components) repeatedly came off after the heating the silicon oil. In order to remove the silver paste after the measurement the samples are dipped into acetone and the paste is slightly wiped off.

The poling process itself sometimes didn't work properly. Either it was not possible to reach the desired value of field strength at elevated temperature, or the voltage gradually went down during the procedure. Especially the BaTiO₃ composites were nearly impossible to polarize and consequently performed poorly at magnetoelectric measurements. One reason might be

a gradient of density caused by the axial pressing process enabling electric sparks through holes in the material. However also with isostatically pressed samples the poling didn't work all the time.

3.1.8 Magnetic Characterization

The magnetization of the composite samples was determined by means of a pulse field magnetometer PFM (Hirst Industrial Systems), seen in Fig. 3.1.9. This pulsed field magnetometer allows a very fast measurement of the magnetic hysteresis loop. A condenser battery is charged up to several kV and subsequently discharged through the magnet. The pulse duration is determined by the inductance L and the capacitance C and was in our case 50 ms. Detailed information about the system can be found elsewhere [59].

The charging process and data acquisition are performed using a Z80 microprocessor linked to a PC. After an analogue integrator the signals are processed through a two channel ADC card from Dattel (model PCI-414N) and finally handled by means of a LABVIEW program. For a correct measurement a zero signal is obtained and subtracted from the sample signal.

3.1.8.1 Analysis of magnetization measurement data

Because of the relatively low sample mass of 0.2-0.4g the "J-Amp"-setting in the LABVIEW software is set to MAX (15000) in order to get suitable results. The raw data of magnetic field and magnetization have to be multiplied with certain calibration factors. For the magnetic field [T] the k-factor [T/V] is $1757.62 / (1/RC\text{-setting "H-amp"})$ whereas for the magnetization the M-factor [emu/V] is $1.95075 \times 10^6 / (\text{J-Amp-setting})$. The resulting value is divided by the mass of the respective sample in order to get the magnetization [emu/g].

3.1.9 Magnetostriction Measurements

Linear magnetostriction was measured by a strain gauge method using a 50 kHz bridge (HBM Type KWS 85A1). Two different types of strain gauges

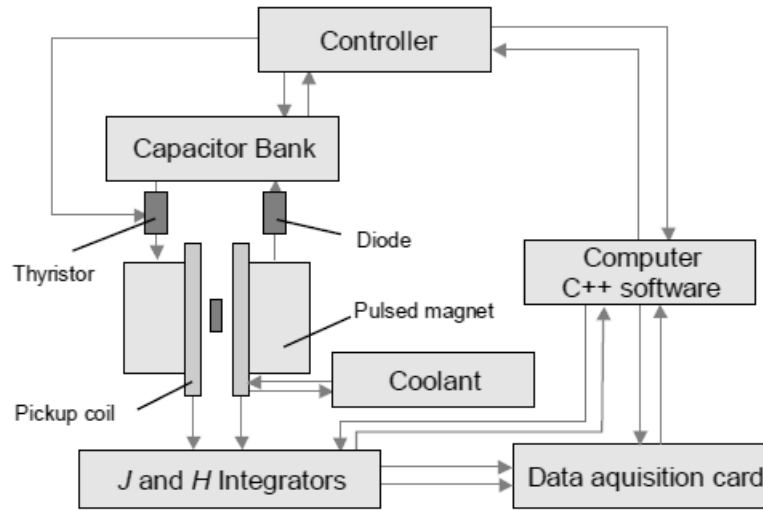


Figure 3.1.9: Block-diagram of the Hirst Magnetometer. Charging of the Capacitor Bank up to 5 T and discharging through magnetic coils induces a pulse field. Magnetic signals are collected by the Pick-Up coils and processed through a data acquisition card to a PC. [59]

were used for the experiments. The Vishay L2A-06-062LT-350, shown in Fig. 3.1.10, has two separate strain gauges aligned in a 90 degree angle allowing to measure both longitudinal and transverse magnetostriction without moving the sample and just switching between the two circles. The HBM 1-LY11-1,5/120 (see Fig. 3.1.11) is a single strain gauge and was used as well (for samples CFPZT_12-14). Here the sample itself is turned 90 degrees between longitudinal and transverse magnetostriction measurement.

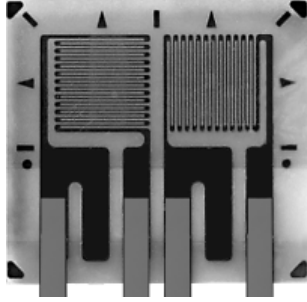


Figure 3.1.10: Vishay double strain gauge [60]

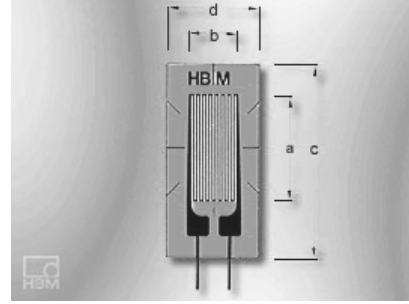


Figure 3.1.11: HBM strain gauge [61]

The attachment of strain gauges requires a clean sample surface. Ethanol or acetone work as cleaning fluid. A small drop of HBM Z70 adhesive glues the strain gauge to the sample. The strain gauge is connected to electric contacts of the sample holder and the sample itself has to be fixed with adhesive tape, otherwise a movement during the magnetic pulse would falsify the results.

The sample holder is placed in the same pulsed magnetic field, described in section 3.1.8. The vertical position of the sample holder can be adjusted and is set to 12.25 on the corresponding scale, putting the sample in the center of the magnetic coil. The system is charged up to 1 kV providing a magnetic pulse of about 2 Tesla with pulse duration of 50 ms. During the charging process the bridge must be continuously adjusted to zero in order to gain a valuable signal curve. In response to the magnetic pulse the sample changes its dimension of length causing a change of resistance in the strain gauge. The corresponding change of the output voltage is proportional to the linear magnetostriction.

A short acetone bath enables the detaching of strain gauges and excessive glue in combination with paper wipes and forceps.

3.1.9.1 Analysis of Magnetostriction Measurement Data

In order to get presentable results the raw data has to be processed. We used the data processing software Origin 7.5. The calibration factor for

the magnetic field is 3.51524 T/V and the magnetostriction data has to be multiplied by a factor F in order to gain the desired dimension of parts per million [ppm].

$$F = 100 \times \frac{2}{k}$$

The strain sensitivity k of a strain gauge is the proportionality factor between the relative change of the resistance and mechanical stress. It can be found in the technical data sheet delivered with each strain gauge package as a nominal value with its tolerance.

3.1.10 Magnetoelectric Characterization

We used a pulsed field method, described in section section §2.2, to determine the magnetoelectric nature of our composite samples. The polarized and silver coated sample discs are fixed in the sample holder. For smaller samples one or two contact pins on the surface are sufficient. The sample holder's vertical position in the measurement system is set to 13.20 on the corresponding scale, see Fig. 3.1.12. However later experiments will show that the position in the magnetic coil has no significant influence on the magnetoelectric performance. The magnitude of magnetoelectric response to the exposure to a magnetic field allowed us to measure without signal amplification for most samples. Therefore the charge amplifier delivered an output voltage directly proportional to the generated charge. This is reached by setting the range capacitor to 1000 pF. The output voltage is processed exactly like the magnetization and magnetostriction signals by means of a ADC card (Dattel model PCI-414N). As for magnetostriction measurements the pulse system is charged up to 1 kV with corresponding magnetic pulse of about 2 Tesla.

The pulse duration of 50 ms requires the operation of the charge amplifier in "short-mode". Although even here a drift of the signal can be observed. Therefore we switched the amplifier on immediately before the discharging process of the battery. The magnetoelectric coefficient most commonly published can be determined as follows

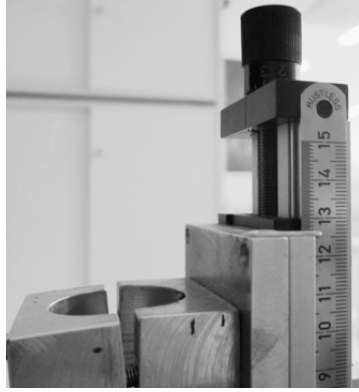


Figure 3.1.12: Height adjustment for the Hirst PFM. The scale corresponds to the vertical position of the sample holder in the field.

$$\alpha_E = \frac{V}{H \cdot d}$$

where V [mV] is the voltage across the sample, H [Oe] is the magnetic field and d [cm] is the thickness of the sample disc.

Chapter 4

Results and Discussion

4.1 Composites of CoFe_2O_4 and BaTiO_3

The original objective of this work was the improvement of the work of Dr. Giap [46] who was the first in the group of Prof. Groessinger to synthesize and measure magnetoelectric composites of CoFe_2O_4 and BaTiO_3 . Through different synthesis routes for Cobalt Ferrite the magnetostrictive component of the composite should be optimized, thus enabling a stronger magnetoelectric performance.

Several months of work gave new and surprising insights into the complexity of driving mechanisms in magnetoelectric composites. Along our way to improvement of ME performance we faced some unexpected obstacles.

4.1.1 CFBT_01-CFBT_03

The first three composites were synthesized via a sol-gel method, described in section 3.1.2. For samples 01 and 02 unsintered Cobalt-Ferrite (sol-gel-method) was introduced during the gelating process whereas for sample 03 a sintered product was used. The resulting powders were pressed into discs of 10mm diameter and sintered at 1000°C for 12 hours.

At first the X-ray diffraction patterns were studied by means of the analyzing software TOPAS 2.0. Quantitative Rietveld analysis delivered some interesting insights. For all samples a cubic spinel structure of Cobalt Fer-

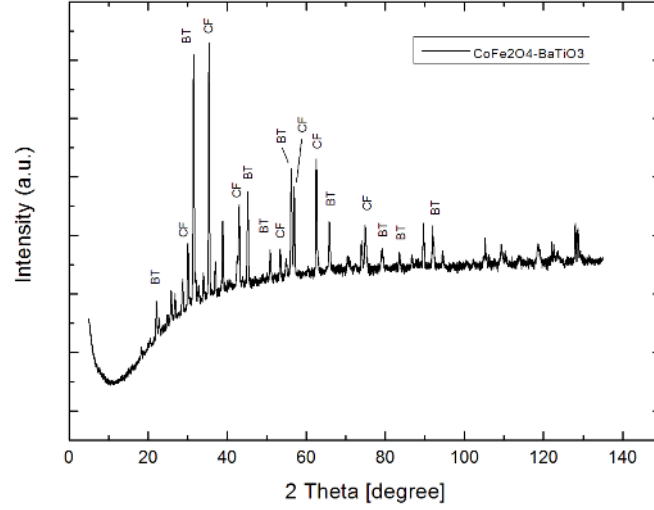


Figure 4.1.1: XRD-pattern of CoFe₂O₄-BaTiO₃ composite CFBT 01

rite, as well as the ferroelectric tetragonal perovskite structure of Barium Titanate, was confirmed.

CFBT01 was sintered in a non-closed crucible and somehow polluted with Sulfates from the furnace surroundings during the process, therefore a variety of different compound phases was found besides the expected Cobalt Ferrite and tetragonal Barium Titanate. Fig. 4.1.1 shows the XRD pattern of the composite with characteristic reflection peaks related to both constituents. The non-identified peaks indicate existence of additional unwanted phases messing up the purity of the composite.

From a crystallographic point of view there was no significant difference between samples 2 and 3. Although originally synthesized at a 1-1 ratio of magnetostrictive and piezoelectric phase, the CoFe₂O₄ percentage was at 60% while tetragonal BaTiO₃ and a small part of BaFe₂O₄ developed during the synthesis process at 35% and 5% respectively. The Rietveld analysis however is not an exact quantitative method and allows just rough estimation of the sample composition.

According to the results of X-ray powder diffraction samples 2 and 3

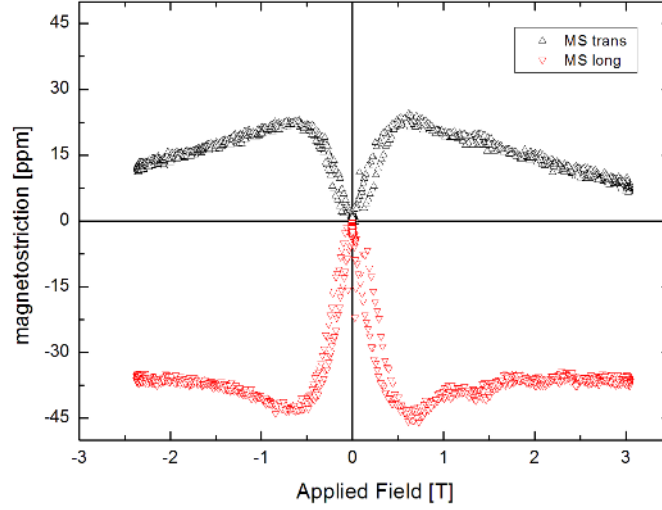


Figure 4.1.2: Longitudinal (red) and transverse (black) magnetostriction of CFBT_01 at 3 T

the chemical synthesis was successful and provided sufficient material for magnetic and magnetoelectric experiments.

Magnetostriction measurements were executed, as described in section 3.1.9. HBM Type KWS 85A1 strain gauges were used for determining longitudinal and transverse magnetostriction of the respective samples.

In comparison to previous experiments in our group by Giap and others we observed a slight improvement of magnetostriction by about 10-20 ppm. As presented in Fig. 4.1.3 and Fig. 4.1.4 samples 2 and 3 present an anomaly since the transverse magnetostriction is higher than the longitudinal one.

4.1.2 CFBT_04-CFBT_07

The production technique varied for each sample. The used cobalt ferrite was used in presintered and non-presintered form and was produced via a standard ceramic-ball milling routine [62] or the sol-gel process described in section 3.1.1.

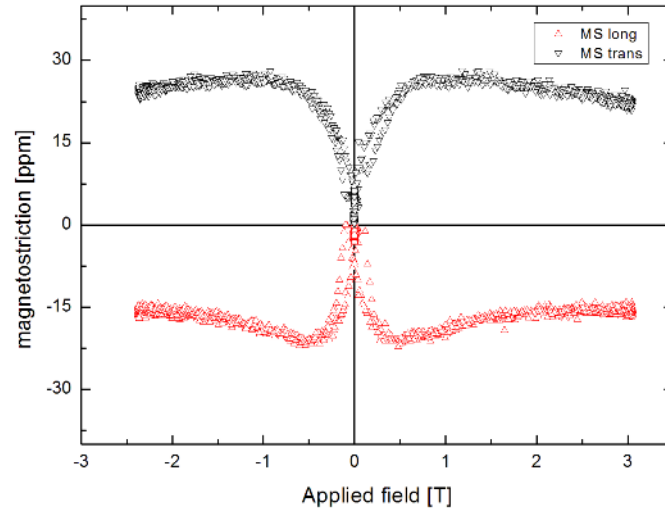


Figure 4.1.3: Longitudinal (red) and transverse magnetostriction (black) of CFBT₀₂ at 3 T

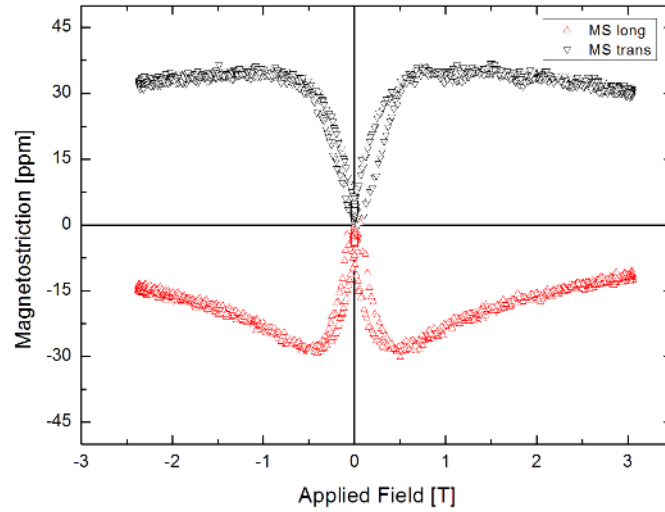


Figure 4.1.4: Longitudinal (red) and transverse (black) magnetostriction of CFBT₀₃ at 3 T

CFBT_04: The sol-gel routine for Barium-Titanate was done in an ultrasonic bath instead of a heating plate with a magnetic stirrer like in the previous experiments. As magnetostrictive component Cobalt Ferrite gained through ball-milling without presintering was used. The resulting powder was sintered at 1000°C for 12h. XRD-Analysis revealed successful synthesis of a composite with 54% CoFe_2O_4 and 45% tetragonal BaTiO_3 and some undefined structures, probably BaFe_2O_4 .

CFBT_05: Same routine as sample 04 but the Cobalt Ferrite (ball-milled) was presintered at 1000°C for 4 hours. The composite showed three different phases in XRD-analysis: 44% CoFe_2O_4 , 54% tetragonal BaTiO_3 and 2% BaFe_2O_4 .

CFBT_06: The powder of sample 04 was hydrostatically pressed at a pressure of 200 MPa and then sintered at 1250°C for 12 hours. The goal was to gain a higher and more homogenous material density opposite to the usual axial pressing method. XRD powder diffraction showed: 35% CoFe_2O_4 , 29% tetragonal BaTiO_3 as well as 36% BaFe_2O_4 .

CFBT_07: Again the synthesis was performed in an ultrasound bath. A sol-gel combustion routine followed by 12 hour sintering at 1000°C provided the Cobalt-Ferrite constituent. Here the XRD analysis unfolded a mixture of four different phases in the composite: 46% CoFe_2O_4 , 25% tetragonal BaTiO_3 , 25% BaTi_2O_5 and 5% $\text{BaFe}_{12}\text{O}_{19}$.

The lattice constants derived from Rietveld analysis are shown in Tab. 4.1

Obviously the hydrostatic pressing and higher sintering temperature enable additional compounds of Ba and Fe to develop, which is not suitable for our purposes. A larger lattice constant a in cubic Cobalt Ferrite however is assumed to provide better magnetostrictive performance. The sol-gel derived CoFe_2O_4 although presintered seems to be more chemically active allowing four different phases to develop during sintering.

Sample	Lattice-Constant (Å)		
	CF (cubic)	BT (tetra)	
	a	a	c
CFBT_01	8.393	4.0057	4.0059
CFBT_02	8.387	4.0069	4.0151
CFBT_03	8.382	4.0042	4.0098
CFBT_04	8.387	4.0063	4.0171
CFBT_05	8.383	4.0041	4.0078
CFBT_06	8.397	4.01	4.004
CFBT_07	8.383	4.0003	4.0078

Table 4.1: Structural parameters of CF-BT composites according to Rietveld analysis of XRD-powder diffraction

4.1.3 Magnetoelectric Measurements

Constantly occurring problems during the polarization process resulting in zero or in some cases hardly measureable magnetoelectric effect, made experimental approaches from all sides necessary. Only at room temperature a sufficient electric field could be applied. With rising temperature the field strength either gradually decreases to zero or in some cases disrupts suddenly with a cut through even destroying some samples.

The idea of the polarization process is to exceed the Curie-temperature by heating a surrounding oil bath, in case of BaTiO_3 $T_c=120^\circ\text{C}$, while applying an electric field and then cool down in order to “freeze” electric moments in a uniform direction enabling a piezoelectric charge caused by mechanical deformation. Otherwise mechanical stress would just induce small micro charges, statistically eliminating each other. Consequently the impossibility of polarizing the samples makes them improper for magnetoelectric purposes.

Only for hydrostatically pressed CFBT_06 a very small ME response could be measured. Fig. 4.1.5 shows the magnitude of the ME voltage coefficient in orders of $\mu\text{V}/(\text{cm}\cdot\text{Oe})$ - below expected values by a factor of 100.

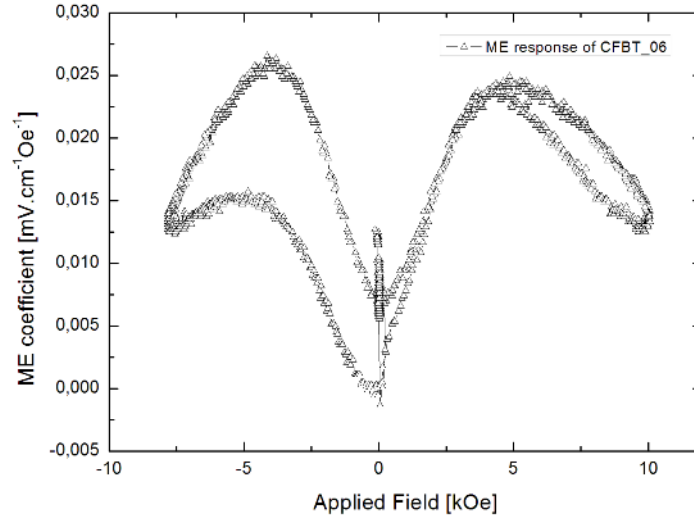


Figure 4.1.5: Small ME response of CFBT_06. ME voltage coefficient α was below expected values by a factor of 100.

4.1.4 Magnetostriction and Magnetic Measurements

Because of constant problems during the polarization process prohibiting any success for magnetoelectric measurements further characterization of the composite materials was not performed in order to save time and money e.g. for strain gauges etc.

4.1.5 Conclusions

Several approaches of synthesizing magnetoelectric composites of magnetostrictive CoFe_2O_4 and ferroelectric BaTiO_3 via a wet chemical sol-gel routine were taken. Although XRD analysis revealed structurally flawless composite material in most cases, hardly no magnetoelectric response could be measured.

The only difference in the production route, compared to literature [23], lies within the synthesis of Cobalt Ferrite, where ceramic ball-milling or sol-gel combustion was used instead of reported co-precipitation. However,

refining the chemical synthesis and improving magnetoelectric performance through enhanced magnetostriction in Cobalt-Ferrite was the original goal of this thesis.

Possible explanations for the surprising results can be found within chemical synthesis and detailed structure of the composite material.

- The often described core-shell structure with magnetostrictive Cobalt Ferrite being surrounded by a matrix of Barium Titanate could not be realized. During chemical synthesis no real gelation could be observed. The Barium-Titanate somehow precipitates in form of white particles of different sizes in the precursor solution during the heating process with Cobalt Ferrite powder being present. Consequently the intrinsic and mechanical coupling between the constituents is not as strong as assumed in a real core-shell structure. Despite the small ME effect, which was measured, our results indicate that the general core-shell theory, reported by Giap, might be questionable and needs further investigation.
- Polarization of the composite samples could not be done successfully, prohibiting any measureable magnetoelectric responses. At room temperature the application of an electric field was possible. However during the heating process, necessary to effectively unify the direction of electric moments, the field either gradually decreased, or a cut-through occurred. Obviously the electric resistance changes with temperature, showing semi-conducting and not insulating character. Complex impedance analysis can offer additional insight in this topic.
- Barium-Titanate itself is a very complicated compound. Although powder diffraction confirmed the desired tetragonal structure a detailed analysis of the material could not be done. Powder diffraction offers just a quantitative idea of a observed material. Accidental doping with iron or cobalt atoms can not be excluded and could heavily influence the dielectric properties. For magnetoelectric composites a soft-ferroelectric material with a low coercivity is suitable, because it is easier to polarize

and shows higher sensitivity to stress. This could neither be confirmed nor ruled out and the semi-conduction features mentioned above make the Barium-Titanate less suitable for our purposes.

As a consequence we approached our goal with a different piezoelectric constituent, namely PZT, in combination with Cobalt-Ferrite for magnetoelectric composite material.

4.2 Composites of CoFe_2O_4 and PZT

PZT is a widely spread material in piezoelectric industry. As Barium Titanate it is a perovskite with the formula $\text{Pb}(\text{Zr}_x\text{Ti}_{1-x})\text{O}_3$ with $0 \leq x \leq 1$. Since the production of such perovskite materials especially with very specific ferroelectric properties is very complex, as observed with Barium Titanate, a new experimental approach utilizing commercially available PZT was tried. The experimental details can be found in section 3.1.3.

A total of 14 different composite samples was synthesized and the influence of stoichiometry, synthesis technique, pressing conditions and sintering temperature on magnetostriction, magnetization and magnetoelectric performance were analyzed.

4.2.1 XRD-Results

As in previous experiments with Barium-Titanate the X-ray powder diffraction was done as a first step. Quantitative Rietveld analysis of XRD-data confirmed three to four different phases in our respective composite samples (space-groups in brackets). Both tetragonal and rhombohedral PZT ceramics show ferroelectric behavior below the Curie Temperature.

- Cubic Cobalt-Ferrite (Fd-3mZ)
- Tetragonal PZT (P4mm)
- Rhombohedral PZT (R3mR)
- Massicot (PbO) (Pbcm)

	CoFe	PZT tet	PZT rhom	PbO
CFPZT_01 (1:1)	56	36	8	
CFPZT_02 (2:1)	67	26	7	
CFPZT_03 (1:2)	39	38	23	
CFPZT_04 (1:3)	31	43	26	
CFPZT_05 (3:1)	81	16	3	1
CFPZT_06 (1:1)	53	38	8	
CFPZT_07 (4:1)	86	7	7	
CFPZT_08 (1:4)	26	58	15	1
CFPZT_09 (9:1)	95	5	0	0.1
CFPZT_10 (1:9)	13	66	21	
CFPZT_11	65	19	16	0.1
CFPZT_12	63	7	30	
CFPZT_13	63	3	33	1
CFPZT_14	62	6	31	1

Table 4.2: weight % of each structural phase according to quantitative Rietveld analysis. The desired ratio of Cobalt-Ferrite:PZT is noted in brackets.

The coexistence of both the rhombohedral and the tetragonal phase in $\text{Pb}(\text{Zr}_x\text{Pb}_{1-x})\text{O}_3$ compounds is well known [63]. The PZT system forms a solid solution with rhombohedral Zr-rich and tetragonal Ti-rich phases with $x \geq 0.52$. The morphotropic phase boundary (MPB) the two ferroelectric phases is almost temperature independent. Above the Curie-temperature however, only a non ferroelectric cubic phase remains.

The analysis however only gives an idea of the phase distribution, the percentages are not exact. According to Tab. 4.2 the preliminary desired ratio of Cobalt Ferrite and PZT was experimentally realized with pleasing success.

Samples 12, 13, 14 were pressed under isostatic conditions, in opposite to axial pressing for all other samples and sintered at 1000°C, 800°C and 650°C respectively. The detailed discussion will follow, but the ratio of tetragonal and rhombohedral PZT dramatically shifted to the latter in comparison to the axially pressed composites.

Generally the count of rhombohedral PZT increases with the amount of PZT in the precursor.

Figure 4.2.1 presents three XRD-patterns of composites with 50:50, 90:10 and 10:90 ratios of Cobalt Ferrite and PZT. The relative intensity of XRD lines depends on the relative abundance of the particular phases in composites. The diffraction patterns of composites reveal that the intensity as well as number of PZT peaks increases with raising its content in the respective sample.

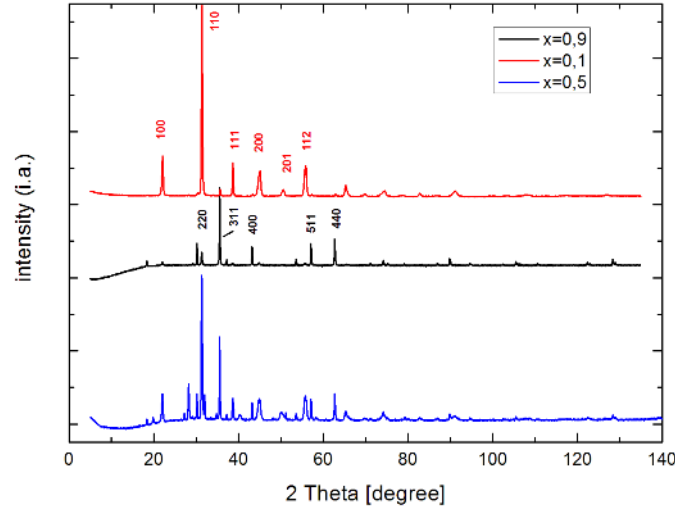


Figure 4.2.1: XRD graph of $\text{CF}_x\text{PZT}_{1-x}$, $0 \leq x \leq 1$, composites with characteristic reflection peaks of PZT (red) and Cobalt Ferrite (black)

Table 4.3 shows structural parameters of sol-gel derived, axially pressed $\text{CF}_x\text{PZT}_{1-x}$ composites sintered at 1000°C for 2 hours. The lattice constant of cubic CoFe_2O_4 increases with the rise of ferrite count in the composite. The lattice parameters of the rhombohedral PZT-phase experience no real influence concerning the ferrite count. The degree of tetragonality of PZT slightly decreases with the reduction of the overall PZT constituent. The lattice parameters are in good agreement with reported values for individual phases in literature [64]. However the slight change of lattice constants

sample	CF	PZT tet			PZT Rhm	
	lattice const.	lattice const.		deg. of tet.		
	a [Å]	a [Å]	c [Å]	c/a	a [Å]	α [°]
x=0,1	8.37	4.04	4.06	1.012	4.05	89.82
x=0,2	8.38	4.03	4.07	1.009	4.05	89.86
x=0,25	8.37	4.02	4.07	1.013	4.05	89.79
x=0,33	8.38	4.02	4.07	1.013	4.05	89.78
x=0,5	8.38	4.04	4.06	1.007	4.04	89.56
x=0,55	8.39	4.03	4.08	1.012	4.05	89.76
x=0,66	8.39	4.03	4.06	1.008	4.05	89.81
x=0,75	8.39	4.04	4.07	1.008	4.05	89.87
x=0,8	8.39	4.03	4.07	1.010	4.05	89.79
x=0,9	8.39	4.04	4.06	1.005	4.05	90.11

Table 4.3: Structural parameters calculated from X-Ray Diffraction for $\text{CF}_x\text{PZT}_{1-x}$ composites

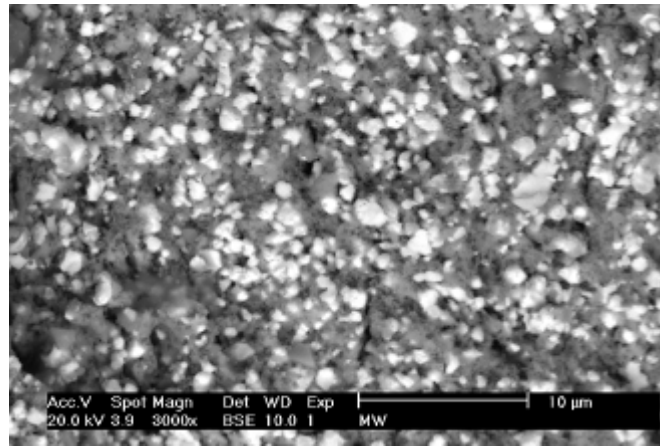
indicates that the Ferrite and PZT phases are strained in the composite, a theory consolidated by the fact that the lattice constant of CoFe_2O_4 shows dependence regarding the content of PZT.

4.2.2 Scanning Electron Microscopy Analysis

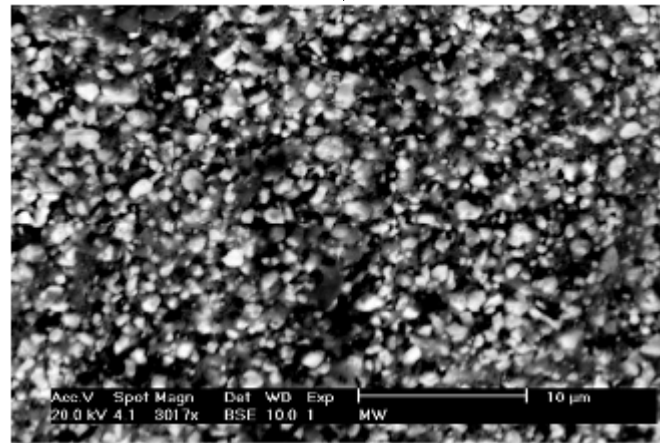
The SEM micrographs of the sample disks fractured inner surfaces were recorded in back-scattered mode. In Fig. 4.2.2 SEM images of three $\text{CF}_x\text{PZT}_{1-x}$ composites are presented, the values of x being 0.5, 0.6 and 0.8 respectively. Two distinct phases occure, a white matrix of PZT and black and grey Cobalt-Ferrite. With x converging to 1 the dark regions become more dominant as expected. The homogenous and well developed fine grains are satisfying and indicate good intrinsic coupling between the constituents. The grain size seems to be well controlled and the grains themselves sufficiently dispersed, underlining the advantages of a sol-gel production routine. Even with increasing the count of Cobalt-Ferrite to 80% the homogeneity prevails and no agglomeration of grains can be observed.

The fact that the grain size of the PZT particles seems to be independent from the count of cobalt ferrite states that the used PZT powder is already

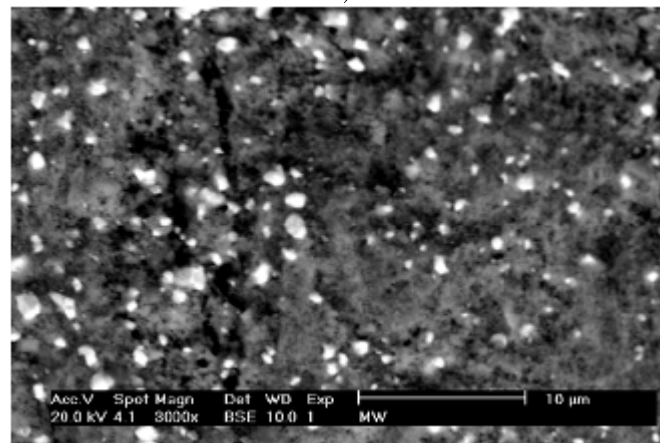
well crystallized. Sintering at 1000°C, necessary for crystallization of the ferrite, has no influence on the material.



a)



b)



c)

Figure 4.2.2: SEM micrographs of $\text{CF}_x\text{PZT}_{1-x}$ composites with a) $x=0.5$ b) $x=0.6$ and c) $x=0.8$

4.2.3 Thermogravimetric Analysis

During the heat treatment of the composite powders several processes such as dehydration and decomposition of organic groups take place. In order to get a better understanding of the sintering step, thermogravimetric analysis was performed on two samples with 50-50 and 67-33 ratios of CF and PZT respectively. The sol-gel prepared powders were heated from room temperature up to 1000°C with a heating rate of 10°C/min. This is three times faster than the heating rate during our sintering process but a lower rate was not possible for the device. The relative weight loss of the samples is pictured in Fig. 4.2.3

Three different weight losses can be observed:

- at about 100°C excessive water evaporates
- between 200-400°C the decomposition of nitrates, citrates and hydroxide or hydroxide-oxides initiates a significant loss of mass. Usually for single phased Cobalt-Ferrite produced via our sol-gel route above 400°C no further losses follow
- above 650°C PbO can partly evaporate a critical step during sintering PZT-ceramics, missing Pb atoms can dramatically change the complex structure and the concurring material properties

With Cobalt-Ferrite being the dominant constituent, the TGA curve shows a decreasing slope, the relative mass loss is higher because more excessive nitrates and citrates decompose as compared to the composite with a higher PZT count. The fact that at 1000°C there still is no sign of a reduced mass loss or even a constant horizontal TGA curve indicates, that there are decomposition processes within the PZT constituent going on. According to the manufacturer, the purchased PZT is sintered at 1250°C in air atmosphere so this seems probable. Since the exact composition of the PZT powder is not known due to industrial confidentiality, the processes at higher temperatures cannot be characterized.

The relative weight loss of about 4.5% up to 400°C is 4-5 times less distinctive than in single phased CoFe_2O_4 prepared by a similar sol-gel synthesis

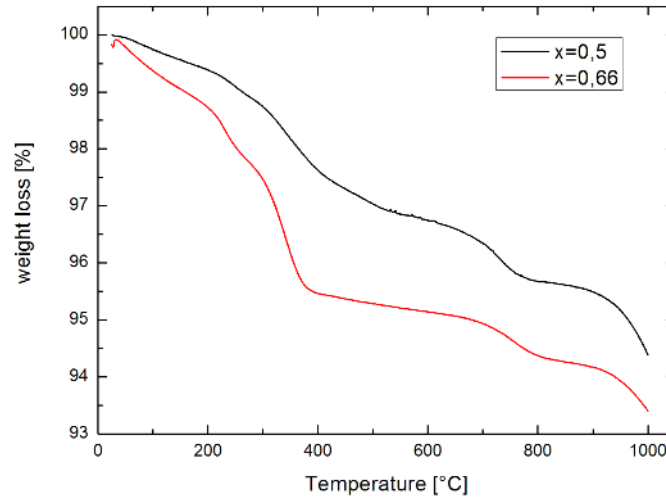


Figure 4.2.3: TGA analysis curve of $\text{CF}_x\text{PZT}_{1-x}$ composites showing the weight loss of the sample powder with increasing temperature. Between 200-400°C the decomposition of nitrates, citrates and hydroxide or hydroxide-oxides leads to a steep gradient in the signal curve. Further weight loss is attributed to evaporation of PbO .

[53].

4.2.4 Magnetic Measurements

Magnetization measurements were carried out on a pulsed field system, described in section 3.1.8. The device provides a very fast way of determining the magnetization at room temperature, however the results can not outmatch measurements done by means of a Vibrating Sample Magnetometer (VSM).

The presented results give a qualitative examination of the magnetic behavior. Exact values for saturation magnetization M_s and coercivity H_c cannot be provided by this method. Fig. 4.2.4 shows a comparison between magnetic measurements by the pulse field system and a Quantum Design Physical Property Measurement System PPMS Q6000 equipped with VSM.

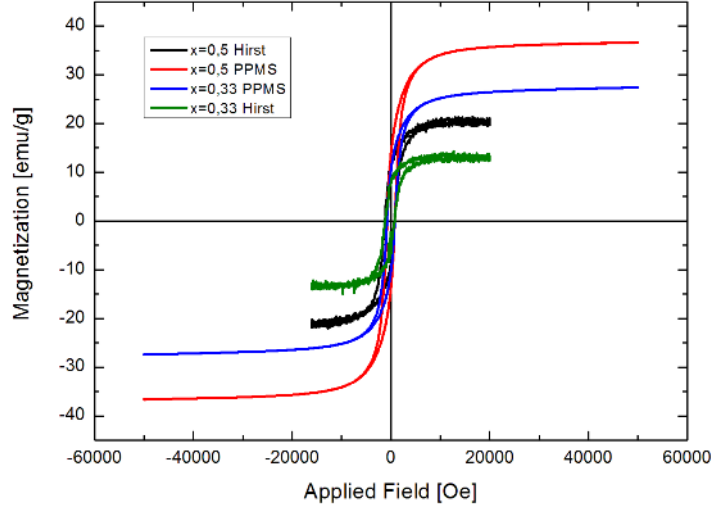


Figure 4.2.4: Magnetic hysteresis of $\text{CF}_x\text{PZT}_{1-x}$ composites determined by a Pulsed Field Magnetometer and a VSM

Clearly the PPMS curves are more refined and the absolute value for magnetization is about 95% higher than with the Hirst Magnetometer. However both methods provide comparable values for the coercive field H_c . For the purpose of this work only relative values for magnetization were relevant, in respect to the ratio of magnetic and non-magnetic constituents. Therefore the Hirst Magnetometer offers sufficient insight into magnetic behavior, although the absolute value for the magnetization is not correct and all results have to be multiplied by a factor of 2.

The saturation magnetization increases with the overall ferrite count in the respective sample. The linear behavior of M_s is presented in Fig. 4.2.5. As the amount of magnetic domains and the interaction in between them decreases with the addition of nonmagnetic PZT the magnetic behavior diminishes with rising PZT count as shown in Fig. 4.2.6.

Although the presented magnetic measurements by a pulsed field magnetometer do not provide quantitatively usable results, as the comparison with curves derived from VMS-measurements points out, we obtain good knowl-

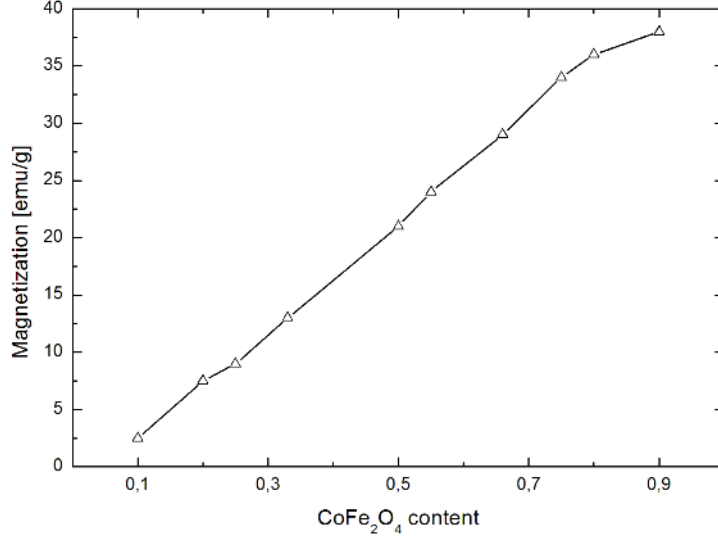


Figure 4.2.5: Saturation Magnetization M_s in $\text{CF}_x\text{PZT}_{1-x}$ composites determined by a Pulsed Field Magnetometer at a field of 20 kOe

edge of the magnetic behavior of our magnetoelectric composites in respect to their composition.

4.2.5 Magnetostriction

Composites of a magnetostrictive and a piezoelectric phase exhibit an electrical charge when exposed to a magnetic field. Good mechanical coupling presumed, a high magnetostriction of the magnetic constituent provides the basis for good magnetoelectric performance. For a large part of this work, starting with composites of CoFe_2O_4 and BaTiO_3 the improvement of magnetostriction was the main goal.

In this section the magnetostrictive behavior of composites of Cobalt-Ferrite and PZT was investigated in regard to a varying ratio of both constituents. Linear magnetostriction was determined in parallel λ_{par} and perpendicular λ_{per} direction of the applied magnetic field. The details for the experimental setup can be found in section 3.1.9.

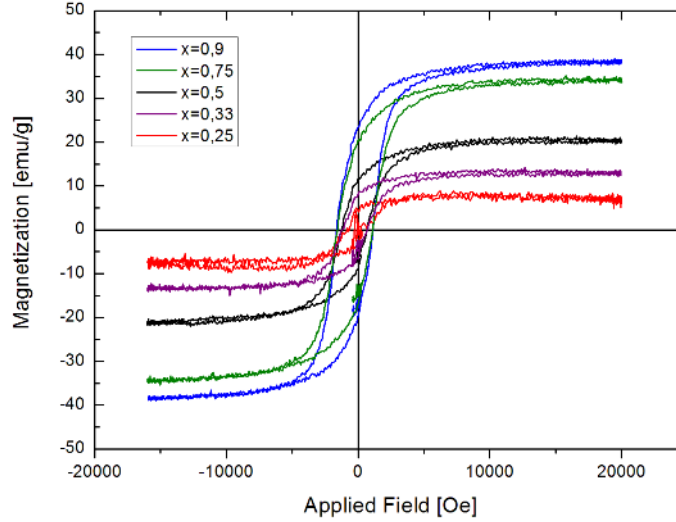


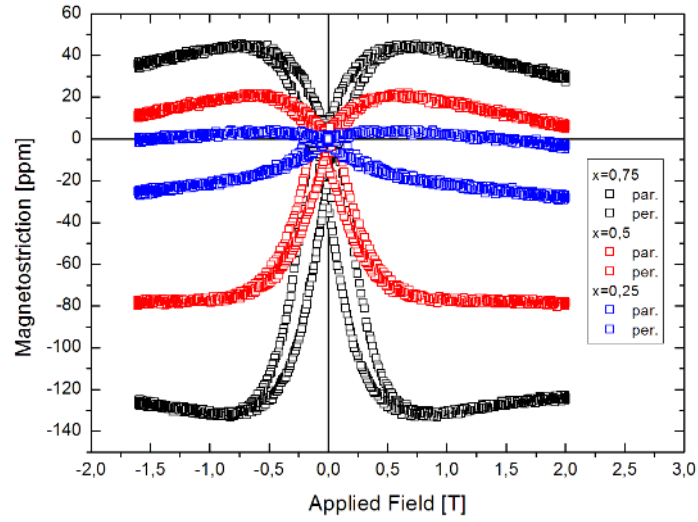
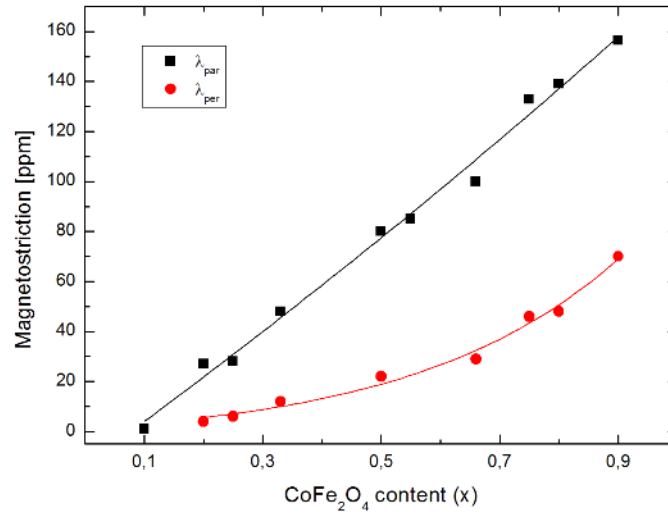
Figure 4.2.6: Magnetic hysteresis of $\text{CF}_x\text{PZT}_{1-x}$ composites. Saturation magnetization M_s rises with increasing amount of magnetic ferrite in the composite.

In Fig. 4.2.7 magnetostriction curves for samples with three different ratios of ferrite and PZT are presented. As expected the linear magnetostriction parallel and perpendicular to the applied field increases with the overall ferrite count in the composite.

The comparison of all prepared composites with x varying from 0.1 to 0.9 can be seen in Fig. 4.2.8.

The addition of PZT to the ferrite obviously changes magnetic and magnetostrictive behavior. The maximum magnetostriction is unsurprisingly found in the composite with maximum ferrite count of 90% with $\lambda_{\text{par}} = -156$ ppm and $\lambda_{\text{per}} = 70$ ppm. Further addition of PZT rapidly decreases magnetostriction.

The fact that less domains react to the applied field and their respective distance also increases with more PZT particles present, explains that behavior. The presence of non-magnetic PZT frustrates the movement of magnetic domains and consequently the change of dimension decreases with a growing amount of PZT. However magnetostriction of these sol-gel derived compos-

Figure 4.2.7: Magnetostriction curves of $\text{CF}_x\text{PZT}_{1-x}$ compositesFigure 4.2.8: Parallel and perpendicular magnetostriction of $\text{CF}_x\text{PZT}_{1-x}$ composites at a magnetic field of about 2 T

Sample	M_s [emu/g]	H_c [Oe]	λ_{par} [ppm]	λ_{per} [ppm]
x=0.1	2.5		1	0
x=0.2	7.5	871	27	4
x=0.25	9	950	28	6
x=0.33	13	914	48	12
x=0.5	21	952	80	22
x=0.55	26	1214	85	
x=0.66	29	1100	100	29
x=0.75	34	1339	133	46
x=0.8	36	1166	139	48
x=0.9	38	1377	156	70

Table 4.4: Magnetic data and magnetostriction for $\text{CF}_x\text{PZT}_{1-x}$ composites

ites is still very large in comparison to samples produced through ball-milling or co-precipitation [65][66].

Parallel magnetostriction λ_{par} of samples prepared by sol-gel synthesis, with a 1:1 ratio of magnetic and ferroelectric constituent is found to be 80 ppm. This exceeds λ_{par} of composites prepared through co-precipitation by 70% and ball-milling by 25% respectively.

Table 4.4 reviews all results from magnetization and magnetostriction measurements for composite samples with varying ratio of Cobalt Ferrite and PZT. Although magnetic measurements by the pulse field magnetometer do not correspond to the more reliable VSM method a trend for magnetic behavior in regard to the overall count of magnetic material in the composite is observable.

4.2.6 Magnetoelectric Effect in $\text{CF}_x\text{PZT}_{1-x}$ Composites

A new pulsed field method utilizing a charge amplifier for signal processing was used for measuring the magnetoelectric effect in composites of magnetostrictive CoFe_2O_4 and piezoelectric $\text{Pb}(\text{Zr}_x\text{Pb}_{1-x})\text{O}_3$. Experimental details are presented in section 3.1.10. The magnetic field is applied perpendicular to the surface of the sample disks. The resulting ME voltage coefficient is derived from the equation

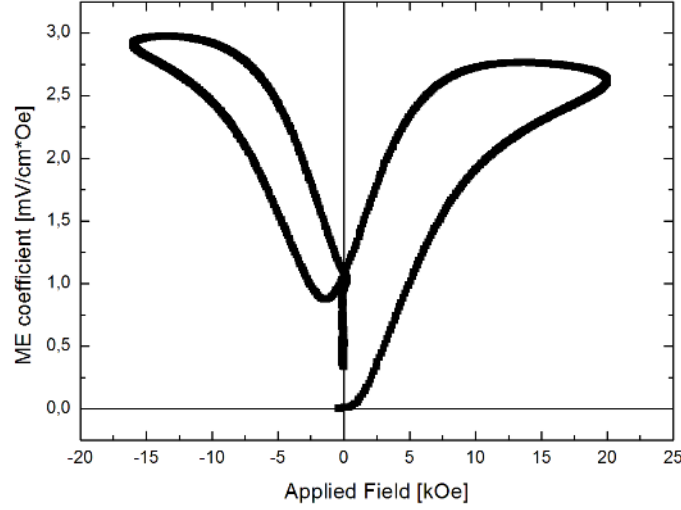


Figure 4.2.9: ME response of CoFe₂O₄- PZT composite (55:45 ratio) to a magnetic field pulse

$$\alpha_E = \frac{V}{H \cdot d}$$

with V being the measured voltage across the sample, H the applied field and d the respective thickness of the sample.

For all samples a field amplitude of 20 kOe was chosen. The ME signal reaches its maximum between 8 and 15 kOe, corresponding to the field strength where magnetization and magnetostriction reach their respective saturation. Applying higher fields does not change the maximum ME response and results in a constant or even slightly declining signal curve until the field breaks down. Since the exhibition of a piezoelectric charge is caused by the magnetostrictive deformation of CoFe₂O₄ the corresponding peak behavior of magnetostriction and ME response seems proper.

As shown in Fig. 4.2.10 the magnetoelectric response is strongly coupled to the magnetostriction. The exhibited charge remains on a constant level with the magnetostriction reaching saturation. Even with the field declining and reaching zero a remanent polarization is observed.

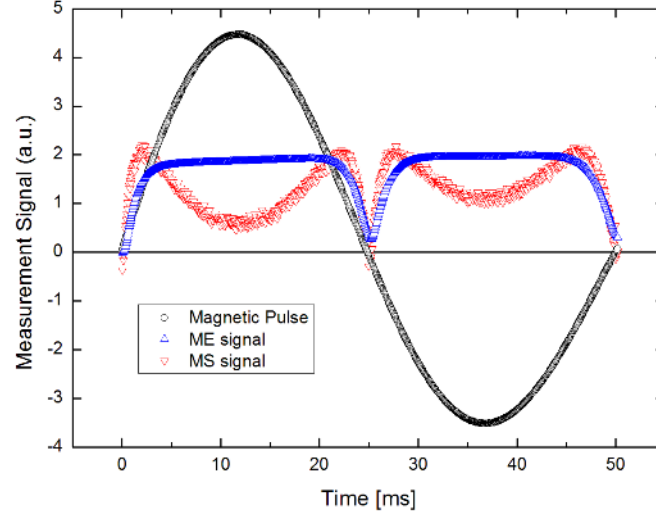


Figure 4.2.10: Measurement signals and magnetic pulse over time

A longer pulse duration or a constant magnetic field would lead to a decrease of the ME signal at some point, since a permanent change of dimension cannot contribute to the piezoelectric effect in PZT.

The magnetoelectric effect in bulk composites is caused by intrinsic mechanical coupling of magnetostrictive and piezoelectric phases. Stress caused by the magnetic pulse induces a change of dimension in the PZT phase and therefore an electric charge occurs. Consequently the molar composition of the composite samples is critical for magnetoelectric performance as presented in Fig. 4.2.11.

The measurement curves follow a similar pattern and reach their respective maximum value at the same field strength.

In Fig. 4.2.12 one can see even more distinctively how the ratio of Cobalt Ferrite and PZT influences the magnetoelectric effect.

The results for the $\text{CF}_x\text{PZT}_{1-x}$ samples with $x=0.5$ and $x=0.66$ indicate an optimal ratio for magnetoelectric performance would be found somewhere in between those compound systems. The sample with 55% Cobalt Ferrite and 45% PZT showed the largest ME response of all synthesized samples

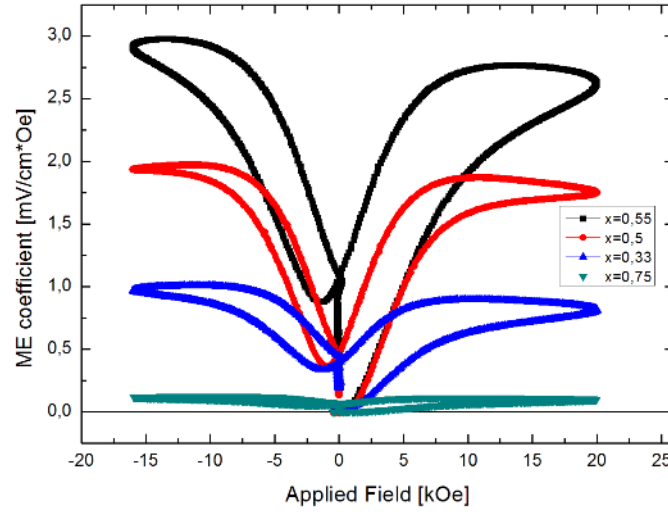


Figure 4.2.11: Variation of the ME coefficient for CF_xPZT_{1-x} composites with different compositions

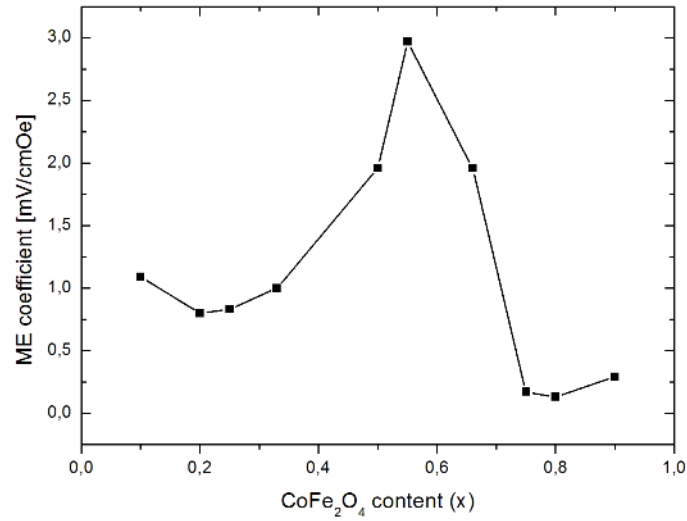


Figure 4.2.12: Dependence of the ME coefficient to the overall count of Cobalt Ferrite in the composite

Sample	α [mV/(cm Oe)]
x=0.1	1.09
x=0.2	0.8
x=0.25	0.83
x=0.33	1
x=0.5	1.96
x=0.55	2.97
x=0.66	1.96
x=0.75	0.17
x=0.8	0.13
x=0.9	0.29

Table 4.5: Magnetoelectric voltage coefficients for $\text{CF}_x\text{PZT}_{1-x}$ composites

with a magnetoelectric voltage coefficient of 2.97 mV/(cm*Oe).

Obviously a decreasing rate of PZT has drastic consequences for the magnetoelectric performance. With less piezoelectric material present, the stress induced charge quickly approaches zero although magnetostriction is of course much higher. However a lower count of Cobalt Ferrite still provides sufficient magnetostriction to cause a piezoelectric response in the dominant PZT-matrix. The fact that at the lowest count of CoFe_2O_4 at 10% even a larger magnetoelectric coefficient is observed can be attributed to the uncertainties of the polarization process.

Table 4.5 lists the magnetoelectric voltage coefficients α for all sol-gel produced $\text{CF}_x\text{PZT}_{1-x}$ composites, axially pressed and sintered at 1000°C.

Multiple composite powders of CoFe_2O_4 and PZT were produced via a wet chemical sol-gel route. The ratio of the respective constituents was varied in order to find the ideal composition for maximum magnetoelectric response. At 55% Cobalt-Ferrite and 45% PZT a maximum magnetoelectric voltage coefficient of 2.97 mV/(cm*Oe) was measured. This is a rather high value for magnetoelectric bulk composites compared to recently published literature.

4.3 Effect of processing parameters on the ME coefficient

In addition to the stoichiometry also certain steps in the synthesis were varied. Axially pressed discs usually suffer a lack of homogeneity in density due to the fact that the powder is pushed to the side by the pressure stamp. Therefore the disc is more dense towards the center than the edges.

In order to provide a homogenous pressing procedure a hydrostatic press (P.O. Weber PW40) was used to produce three cylindrically shaped pellets of approximately 8 mm diameter and 4 mm height. We pressed composite powder with a 1:1 ratio of Cobalt Ferrite and PZT at 320 MPa.

The samples underwent heat treatment at three different temperatures. The first one was sintered at 1000°C like the axially pressed samples. The second one should be sintered at 800°C for 2 hours and the heating rate was 3.2°C/min and cooled down naturally for about 10 hours. Due to problems with the furnace the cooling process was not initiated and consequently the sample was kept at 800°C for more than 12 hours. The third sample was sintered at 650°C for 5 hours and a respective heating rate of 3.5 °C/min and also cooled down naturally. Afterwards the samples were cut into discs of about 1mm thickness, coated with silver paste and polarized.

XRD-analysis revealed different results for hydrostatically pressed composite samples. As stated in section 4.2.1, the count of rhombohedral PZT drastically increased whereas the count of tetragonal PZT fell below 10% in opposite to the axially pressed samples. Especially in sample CFPZT_13 (sintered at 850°C) only two percent of the PZT material showed the tetragonal structure.

Obviously isostatic pressing favors the formation of rhombohedral PZT regardless of the sintering temperature according to Tab. 4.6. The temperature itself seems to have no significant impact on the stoichiometric composition of the material.

The higher count of the rhombohedral PZT phase changes the structural parameters of the tetragonal PZT. Once again the sintering temperature does not seem to significantly influence the structure, only in CFPZT_13 which

Sample	CoFe	PZT tet	PZT rhom	PbO
CFPZT_12 (1000°C)	63	7	30	
CFPZT_13 (800°C)	63	3	33	1
CFPZT_14 (650°C)	62	6	31	1
CFPZT_01 (axially pressed)	56	36	8	

Table 4.6: weight % according to quantitative Rietveld analysis of hydrostatically pressed composite powder with a 1:1 ratio of CF and PZT

sample	CF	PZT tet			PZT Rhm	
	lattice const.	lattice const.		deg. of tet.		
	a [Å]	a [Å]	c [Å]	c/a	a [Å]	α [°]
CFPZT_12	8.38	4.00	4.08	1.02	4.04	90.21
CFPZT_13	8.38	4.02	3.99	0.99	4.04	89.87
CFPZT_14	8.38	4.01	4.08	1.02	4.04	89.88
CFPZT_01	8.38	4.04	4.06	1.01	4.04	89.56

Table 4.7: Comparison of structural parameters calculated from XRD-analysis for isostatically and axially pressed CF-PZT composites with respective 1:1 ratio

was sintered at 800°C for more than 12 hours instead of 2 a serious effect on the lattice constants of the tetragonal phase are obvious.

Hydrostatic instead of axial pressing changes the dominant PZT structure from tetragonal to rhombohedral. The structural parameter themselves seem to be independent from pressing procedure and sintering temperature which is surprising since usually sintering temperature strongly corresponds with lattice constants and crystallite size.

4.3.1 Magnetic and Magnetostriction Measurements

The sintered samples were cut into discs of about 1mm thickness for measurement and also comparison reasons. The measurement process itself was exactly the same as for all other samples.

Magnetic hysteresis curves hardly differ from the axially pressed composites, however for the sample sintered at 650°C the coercive field is reduced by about 50% compared to higher temperatures as shown in Fig. 4.3.1.

Magnetostriction measurements revealed that isostatic pressing leads to

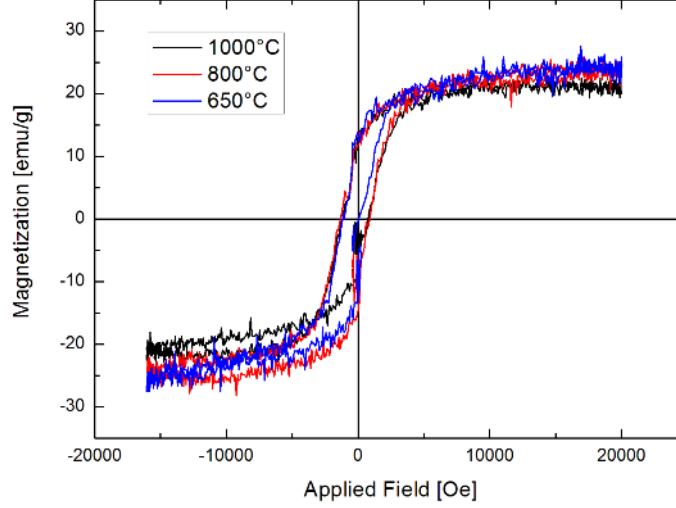


Figure 4.3.1: Magnetic hysteresis of isostatically pressed CF-PZT composites sintered at 1000°C, 800°C and 650°C

a reduction of longitudinal MS of about 15%, however the transverse MS increases by 2%. Equal results for samples sintered at 1000°C and 800°C are obtained, whereas further reducing of the sintering temperature results in a significant drop in magnetostriction, see Fig. 4.3.2. This meets general expectations because higher temperatures favor formation of larger crystallite sizes thus generating a stronger magnetostrictive response to an external field.

All magnetic and magnetostrictive data for isostatically pressed composites of 50% Cobalt Ferrite and 50% PZT are reviewed in Tab. 4.8. Isostatic pressing does not seem to offer improvement compared to axial method from a magnetic point of view. The magnetic hysteresis curve shows similar behavior however the far more important magnetostriction drops significantly.

4.3.2 Magnetoelectric Measurements

The sample discs were coated with silver paste and the polarization procedure followed. Similar to the attempts with BaTiO₃ several unexpected issues occurred during this process. For sample CFPZT_12 the electric field of

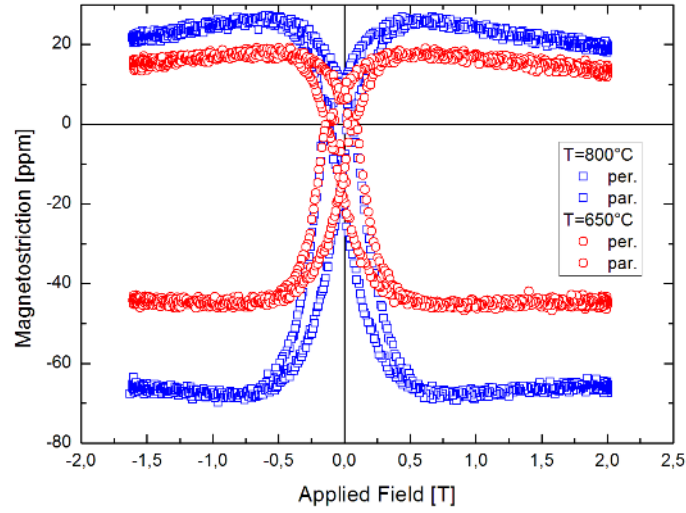


Figure 4.3.2: Longitudinal and perpendicular MS for isostatically pressed CF-PZT composites sintered at 800°C and 600°C

Sample	M_s [emu/g]	H_c [Oe]	λ_{par} [ppm]	λ_{per} [ppm]
CFPZT_12	21	1112	68	26
CFPZT_13	24	1112	68	26
CFPZT_14	24	629	45	18

Table 4.8: Magnetic data and magnetostriction for isostatically pressed CF-PZT composites

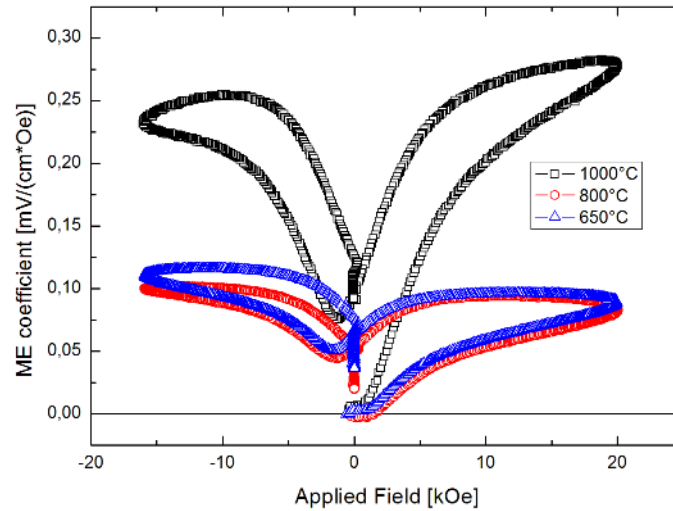


Figure 4.3.3: Magnetoelectric effect in isostatically pressed CF-PZT composites sintered at 1000°C, 800°C and 650°C

about 0.5 kV gradually went down with rising temperature. However it did not break down completely because a relatively high amount of amperage was applied in addition to the voltage. For insulating materials this is surprising.

For CFPZT_13 the application of a high voltage field was not possible at all, unexpectedly a small ME signal could be detected despite this fact. CFPZT_14 showed no problems. At elevated temperatures the electric field remained on a constant level and during the cool down it even increased before reaching the initial level at about 50°C.

All samples exhibited an electric charge during the magnetic field pulse, however the magnetoelectric voltage coefficient is outmatched by a factor of 10 compared to the axially pressed composites as displayed in Fig. 4.3.3.

4.3.3 Conclusions

Isostatic instead of axial pressing provides more dense sample discs with no density gradient towards the edges. However the high pressure of 278 MPa compared to about 22 MPa at axial pressing has a great influence on the

magnetostrictive and consequently on the magnetoelectric behavior. Additionally to the pressing parameters also the sintering temperature was varied.

Structural changes in the composite material are observed since isostatic pressing obviously favors the formation of rhombohedral instead of tetragonal PZT. The structural parameters of the ferrite phase seem to experience no significant influences. Whereas magnetization curves show similar behavior for both pressing methods the longitudinal magnetostriction suffers a serious drop of about 15%. For sintering temperatures below 800°C these losses are even stronger, probably because only high temperatures enable formation of larger crystallite sizes benefiting high magnetostriction.

Because of the drop in magnetostrictive performance also a weaker ME signal was expected since those effects strongly correspond. However the magnetoelectric signal decreased by an even larger factor. Obviously the problems during the polarization step have to be taken into account, however a possible explanation for the non insulating behavior at temperatures above 100°C is difficult to find.

In a recently published work of Groessinger and Muhammad [67] the influence of hydrostatic pressure on the magnetostriction of CoFe_2O_4 is examined. According to the authors, magnetostriction reaches a maximum for powder pressed at 167 MPa and rapidly decreases for higher pressures. This coincides with our experiences and further experiments, suggesting that lower pressure could offer more promising results.

Reducing the temperature for the sintering step had a negative influence on both magnetostriction and consequently the ME output. At lower temperatures evaporation of larger amounts of PbO is prevented, however according to TGA-analysis this is not a serious problem for temperatures up to 1000°C. Again experiments with even higher temperatures should be taken into consideration.

4.4 Influence of phase connectivity on the ME effect

The connectivity of the magnetostrictive and the piezoelectric constituent of a magnetoelectric composite is crucial for the ME performance. The mechanic strain in the ferrite caused by the application of an external magnetic field must be transferred to the piezoelectric phase in order to generate an electric charge. Good intrinsic connection in between the two respective phases lays the foundation for a high magnetoelectric output.

In order to demonstrate the necessity of strong interphase coupling other synthesis routes than our sol-gel routine were looked upon. The probably most derivative way to synthesize a magnetoelectric composite is to mechanically mix the two constituents CoFe_2O_4 and PZT together in a mortar.

Equal amounts (0.45g) of sol-gel derived Ferrite and PZT were grinded together for about five minutes until a visual homogenous powder was obtained. The resulting material showed more shades of brown than the black-grey sol-gel samples. The final powder was processed exactly like all other samples: pressed into a pellet, sintered at 1000°C and then characterized through XRD, SEM, magnetic, magnetostriction and magnetoelectric measurements.

4.4.1 Structural Analysis and SEM studies

X-Ray Diffraction patterns along with Rietveld analysis revealed similar results for both synthesis methods as shown in tables 4.9 and 4.10.

Sample	CoFe	PZT tet	PZT rhom
mixed powders	53	38	9
sol-gel	56	36	8

Table 4.9: weight % according to quantitative Rietveld analysis for $\text{CF}_x\text{PZT}_{1-x}$ ($x=0,5$) composites prepared by different methods

From a structural point of view there seems to be no significant difference between composites derived from sol-gel synthesis and mechanically mixed powders. SEM imaging however unfolds a huge divergence in morphology

sample	CF	PZT tet			PZT Rhm	
	lattice const.	lattice const.		deg. of tet.		
	a [Å]	a [Å]	c [Å]	c/a	a [Å]	α [°]
mixed powders	8.38	4.04	4.06	1.01	4.03	89.47
sol-gel	8.38	4.03	4.06	1.01	4.04	89.56

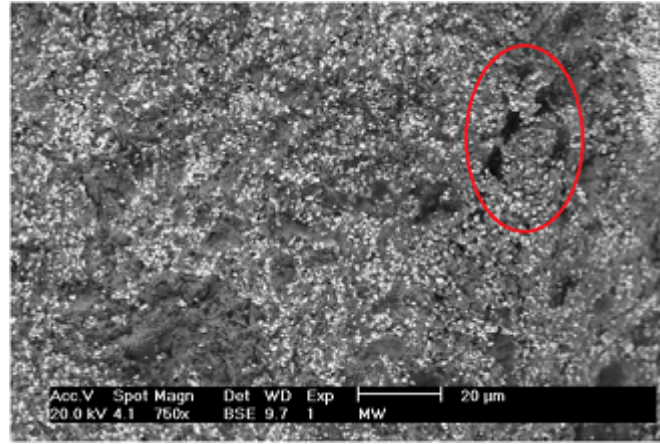
Table 4.10: Structural parameters of $\text{CF}_x\text{PZT}_{1-x}$ ($x=0,5$) composites prepared by different methods

for the two methods. The sol-gel sample shows a homogenous dispersion of black/grey ferrite surrounded by white PZT particles as well as good densification. For the mechanically mixed sample however clearly a lack of homogeneity and even the existence of pores are obvious (see Fig.4.4.1a). Aggregates of accumulated Cobalt Ferrite demonstrate a poor distribution of phases (Fig. 4.4.1b). The fact that the grain size and dispersion of the white PZT particles is the same in both samples indicates that the well crystallized material is not influenced by the chemical processes during the sol-gel synthesis. Hence the sol-gel route produces a superior composite material compared to mechanical mixing. The lack of homogeneity as well as densification suggests a loss of connectivity between the magnetostrictive and the piezoelectric phase consequently having a impeding effect on the magneto-electric performance.

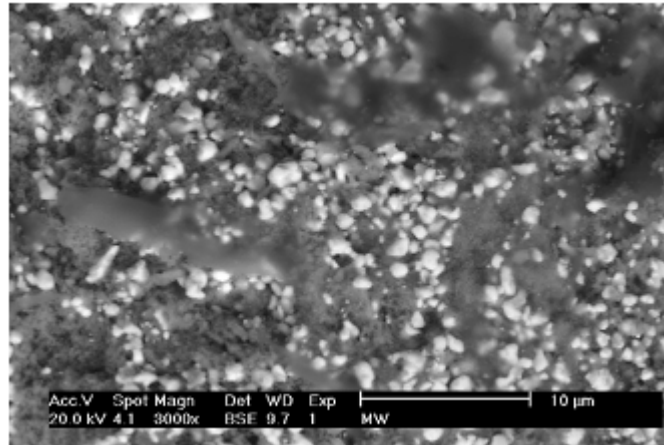
4.4.2 Magnetic and Magnetoelectric Characterization

Both composite powders experienced equal processing in terms of pressing, sintering, polarization and measurement setups. Magnetic hysteresis shows an almost identical curve progression which is not at all surprising since an equal amount of magnetic ferrite material was used for the respective samples. (see Fig. 4.4.2)

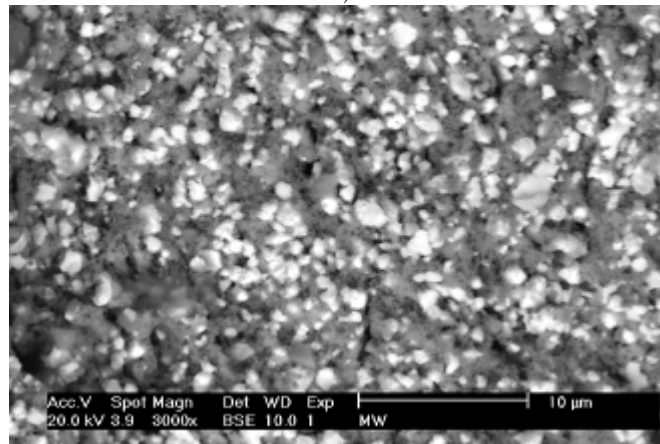
Magnetostriction is a local phenomenon measured directly at the surface where the strain gauge is attached. Consequently a non homogenous distribution of magnetostrictive particles prohibits a general information of magnetostrictive behavior. SEM micrographs clearly indicate the lack of homogeneity in the distribution of magnetic and piezoelectric constituents



a)



b)



c)

Figure 4.4.1: SEM micrographs of a) and b) mechanically mixed $\text{CF}_x\text{PZT}_{1-x}$ ($x=0.5$) composites compared to c) sol-gel derived material

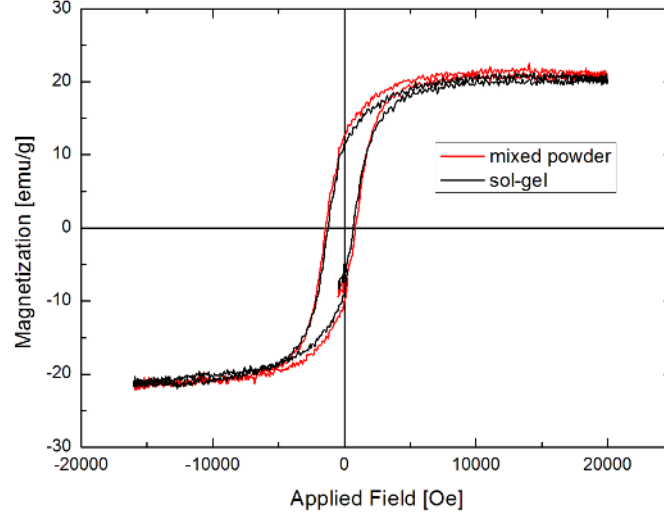


Figure 4.4.2: Magnetic hysteresis of mechanically mixed and solgel derived $\text{CF}_x\text{PZT}_{1-x}$ ($x=0.5$) composites

(see Fig. 4.4.1). The increase in longitudinal magnetostriction in the mixed composite could suggest chemical influence through the PZT powder in the reaction solution during the sol-gel process resulting in a loss of MS. However only a simultaneous boost in transverse magnetostriction could prove such demeanor. This is obviously not the case, as seen in Fig 4.4.3, and the rise in longitudinal magnetostriction of mixed powder composites is probably due to deficient distribution of ferrite grains. If the strain gauge is attached on a region with a high count of Cobalt Ferrite, consequently the local magnetostriction will be higher. With the used Vishay double strain gauge longitudinal and transverse magnetostriction are measured parallel on different spots on the surface which is suitable for homogenous materials. In this case it confirms the lack of particle distribution in the mechanically mixed composite.

A non homogeneous composite material is not expected to produce an as strong magnetoelectric output as a composite with good particle distribution. Agglomeration of ferrite particles favors a locally higher magnetostriction, as

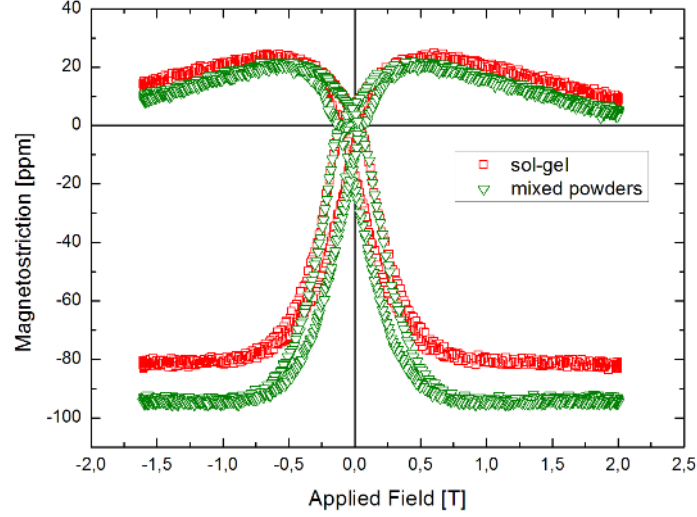


Figure 4.4.3: Longitudinal and transverse magnetostriction of sol-gel and mixed powder composites of $\text{CF}_x\text{PZT}_{1-x}$ ($x=0,5$)

presented, however the magnetically induced strain cannot be transferred to the piezoelectric phase as efficiently. Fig. 4.4.4 presents the the ME voltage coefficients for both synthesis methods. ME performance for the mechanically mixed composite reaches about 50% in magnitude compared to the sol-gel sample.

4.4.3 Conclusion

Magnetoelectric composites of $\text{CF}_x\text{PZT}_{1-x}$ ($x=0,5$) produced via a sol-gel synthesis route and mechanical mixing for were compared. Although the structural parameters according to XRD-analysis seem to be independent from the synthesis, SEM imaging reveals huge difference in homogeneity and particle distribution. Whereas the sol-gel synthesis produces dense, homogeneous and well-developed microstructure, mechanical mixing leads to agglomeration of ferrite- and PZT rich regions and even the formation of pores. Magnetostriction measurements also demonstrate differences in local parti-

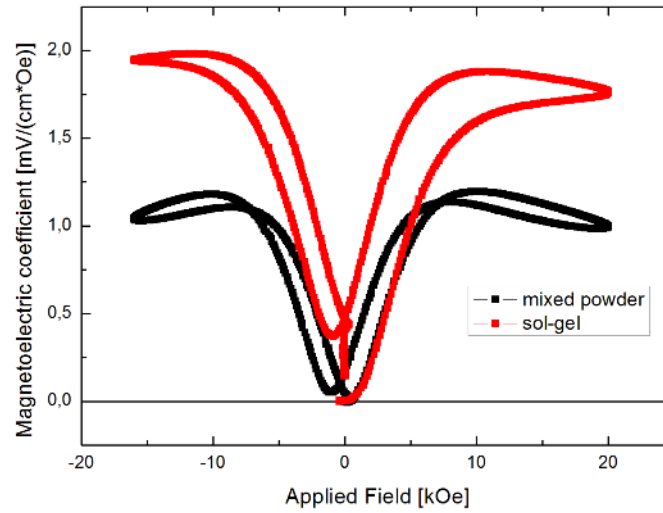


Figure 4.4.4: ME voltage coefficient for composites prepared by mixed powders and sol-gel

cle distribution by delivering non corresponding values in longitudinal and transverse direction. The ME voltage coefficient is reduced to about 50% of the magnitude for the mechanical mixing method underlining the importance of interphase connectivity as well as homogeneity in composite materials.

Even with ceramic ball-milling the ME performance of sol-gel composites cannot be outmatched according to [68]. The sol-gel route for producing spinel Cobalt Ferrite, with PZT particles present in the precursor solution, favors the formation of homogeneous phase distribution and a good connectivity in between magnetostrictive and piezoelectric particles and therefore leads to a superior magnetoelectric performance compared to mechanical mixing or ceramic ball milling.

Chapter 5

Conclusion and Outline

A pulse field method utilizing a charge amplifier has been developed for the magnetoelectric characterization of composite materials of magnetostrictive and piezoelectric constituents. A sample holder for sample discs with varying thickness was designed. The field is generated by a Hirst Industrial Systems pulse field arrangement and applied perpendicular to the sample surface. The pulsed field method eliminates several undesirable side effects occurring with other setups such as frequency dependence and discharging processes and offers a very straight forward measurement approach of the ME effect since the piezoelectric charge induced by the change in dimension in response to the magnetic field is measured directly.

Although the investigation of ME materials has been going on since the early 60's of the last century, still no standardized measurement method has been developed. Therefore only comparisons within our measurement circle are valid and a comparison to experiments of other groups with different measurement setups is difficult, due to non existence of any benchmarks or calibration standard samples.

With the measurement setup established, several approaches for synthesizing magnetoelectric composites combining the product properties of magnetostrictive CoFe_2O_4 and piezoelectric BaTiO_3 or PZT respectively have been carried out. For the spinel Cobalt Ferrite a wet-chemical sol-gel route proved most promising as for the synthesis of Barium Titanate. First exper-

iments targeted towards a formation of a BTO matrix around CFO particles through gelation. Due to precipitation instead of gelation a mixed powder composite was created opposite to the desired core-shell type structure with ferrite as the core. Structural analysis confirmed a two-phase composite of CoFe_2O_4 and BaTiO_3 with small percentage of additional phases.

Addition of BTO consequently lowers magnetization as well as magnetostriction compared to pure Ferrite material, which is of course expected. Longitudinal magnetostriction is still on a sufficient level for good ME output.

Polarizing the samples in an electric field above the Curie-temperature lead to surprising behavior. The resistivity of the composite seems temperature dependent and the desired insulating nature is not accomplished. Therefore magnetoelectric response was extremely low. This is primarily attributed to the BaTiO_3 phase which is probably hard ferroelectric with high coercivity and consequently hard to polarize and not very sensible to small dimensional changes. Therefore a soft ferroelectric material had to be found, for replacing BTO, namely industrial $\text{Pb}(\text{Zr}_x\text{Ti}_{1-x})\text{O}_3$ with $0 \leq x \leq 1$ doped with Ni and Nb.

Introducing the PZT powder into the precursor solution during the sol-gel process for CoFe_2O_4 provided a successful synthesis method for magnetoelectric composites. XRD analysis presented three structures in the final material: cubic CoFe_2O_4 and PZT in rhombohedral as well as tetragonal structure. X-Ray studies also revealed a straining effect of PZT on the lattice parameters of the ferrite phase. Further investigation with SEM microscopy showed a homogeneous composite surface with well dispersed particles.

A wide range of samples was produced in order examine the influence of stoichiometry and synthesis parameters such as sintering temperature or pressing conditions on the magnetoelectric performance. A composition of 55% Cobalt Ferrite and 45% PZT, pressed axially at 6 t/cm² sintered at 1000°C for 2 hours, provided the maximum ME response with 2.97 mV/(cm*Oe). The value dropped significantly with increasing ferrite count, whereas high percentages of PZT still yielded in proper ME output.

Alternatively to the sol-gel route, ferrite and PZT powders were mixed

together mechanically resulting in a less homogeneous and not well dispersed microstructure and a drop of the ME voltage coefficient of about 50%. Connectivity in between the two constituent phases as well as a homogeneous particle dispersion are critical parameters for good magnetoelectric performance.

Isostatic instead of axial pressing eliminated the tetragonal phase of PZT almost completely and the rhombohedral structure was dominant. Additionally polarization lead to similar incidents as the BaTiO₃ samples and the ME output was low especially for sintering temperatures below 1000°C.

Summing up the goals of this thesis were the development and installation of a new pulse field method for detecting the magnetoelectric effect. A charge amplifier was used to collect piezoelectric charges caused by a magnetic pulse. The setup of the measurement system was successful as well as the wet chemical synthesis of magnetoelectric composites of magnetostrictive CoFe₂O₄ and piezoelectric PZT. Hard ferroelectric behavior and poor electric insulation prohibited strong ME response of composites with BaTiO₃ instead of PZT.

For the PZT composites according to TGA analysis even higher sintering temperatures are possible without excessive evaporation of PbO. This could be the next step of further investigation. Also isostatic pressing with lower force could offer performance improvement. Another approach could be polarization at higher temperatures because the Curie temperature of the used PZT powder is 170°C which was never reached in our experiments. Magnetic annealing strongly improves the magnetostriction of cobalt ferrite and therefore would also improve the magnetoelectric voltage coefficient. However through polarization at elevated temperatures magnetic order could suffer a decline again.

For the general investigation of the ME effect the development of a standardized measurement system is desirable in order to obtain a comparability of experimental results. Up to now the influence of the measurement method on the actual result is not well documented. Frequency dependencies allow ME measurements at resonance frequencies and result in huge values for the ME coefficient. Consequently we cannot determine an actual and

commonly legitimate value for the ME coefficient. Hopefully the presented pulse-field method enhances further understanding of magnetoelectric materials and further development in chemical synthesis and sample preparation will certainly improve the ME performance of bulk composites of CoFe_2O_4 and $\text{Pb}(\text{ZrTi})\text{O}_3$.

Chapter 6

Scientific Activities

Journal Articles

R. Turtelli, M. Atif, J. Krippel, R. Grössinger, F. Kubel, W. Linert: "Superparamagnetic CoFe_2O_4 prepared by modified oxalate method"; International Journal of Materials Research, 9 (2012), S. 1163 - 1165.

Conferences and Talks

J. Krippel, A. Muhammad, R. Grössinger, F. Kubel, W. Linert: "Magnetoelectric effect in sol-gel derived $\text{CoFe}_2\text{O}_4\text{-Pb}(\text{ZrTi})\text{O}_3$ composites studied by means of pulsed field method"; Poster: 16. Tagung Festkörperanalytik, Wien; 04.07.2011 - 06.07.2011; in: "Analytical and Bioanalytical Chemistry", Springer, (2011).

J. Krippel, A. Muhammad, R. Grössinger, W. Linert, F. Kubel: "Magnetoelectric characterization of wet chemically synthesized $\text{CoFe}_2\text{O}_4\text{-Pb}(\text{ZrTi})\text{O}_4$ composites by means of a pulsed field method"; Poster: EIC 2011: An International Student Research Conference, New York; 13.04.2011 - 15.04.2011; in: "2011 Einsteins in the City", (2011), S. C.6.

R. Sato Turtelli, M. Atif, J. Krippel, R. Grössinger, F. Kubel, W. Linert: "Superparamagnetic CoFe_2O_4 prepared by modified oxalate method"; Poster: 14th International Conference on Rapidly Quenched and Metastable

Materials, Salvador, Brasilien; 28.08.2011 - 02.09.2011.

Bibliography

- [1] L. Landau, E. Lifshitz, *Electrodynamics of Continuous Media*, Pergamon, Oxford, UK, 1960.
- [2] P. Curie, No Title, *J. Physique* 3 (1894) 393.
- [3] P. Debye, No Title, *Z. Phys.* 36 (1926) 300.
- [4] I. Dzyaloshinskii, No Title, *J. Phys. Chem. Solids* 4 (1958) 121.
- [5] D. Astrov, No Title, *Sov. Phys.* 13 (1961) 729.
- [6] V. J. Folen, G. T. Rado, E. W. Stalder, Anisotropy of the Magnetoelectric Effect in Cr₂O₃, *Physical Review Letters* 6 (1961) 607–608.
- [7] J. van Suchtelen, No Title, *Philips Res. Rep.* 27 (1972) 28.
- [8] J. Van Den Boomgaard, D. Terrell, R. Born, G. H., An in situ grown eutectic magnetoelectric composite material, *Journal of Materials Science* 9 (10) (1976) 1705.
- [9] M. Fiebig, Revival of the magnetoelectric effect, *Journal of Physics D: Applied Physics* 38 (8) (2005) 123–152. doi:10.1088/0022-3727/38/8/R01.
- [10] <http://www.sciencedirect.com>.
URL `www.sciencedirect.com`
- [11] H. Schmid, Multiferroic Magnetoelectrics, *Ferroelectrics* 162 (1994) 317.

- [12] N. A. Hill, A. Filippetti, Why are there any magnetic ferroelectrics?, *Journal of Magnetism and Magnetic Materials* 242-245 (2002) 976–979. doi:10.1016/S0304-8853(01)01078-2.
URL <http://linkinghub.elsevier.com/retrieve/pii/S0304885301010782>
- [13] N. A. Hill, Why Are There so Few Magnetic Ferroelectrics ?, *Journal of Physical Chemistry B* 104 (29) (2000) 6694–6709.
- [14] T. Kimura, T. Goto, H. Shintani, K. Ishizaka, T. Arima, Y. Tokura, Magnetic control of ferroelectric polarization., *Nature* 426 (6962) (2003) 55–8. doi:10.1038/nature02018.
URL <http://www.ncbi.nlm.nih.gov/pubmed/14603314>
- [15] N. Hur, S. Park, P. Sharma, J. Ahn, S. Guha, Electric polarization reversal and memory in a multiferroic material induced by magnetic fields, *Nature* 429 (May) (2004) 392–395. doi:10.1038/nature02568.1.
URL <http://www.nature.com/nature/journal/v429/n6990/full/nature02572.html?fr>
- [16] D. Khomskii, Classifying multiferroics: Mechanisms and effects, *Physics* 2 (2009) 20. doi:10.1103/Physics.2.20.
URL <http://link.aps.org/doi/10.1103/Physics.2.20>
- [17] B. B. Van Aken, T. T. M. Palstra, A. Filippetti, N. a. Spaldin, The origin of ferroelectricity in magnetoelectric YMnO₃., *Nature materials* 3 (3) (2004) 164–70. doi:10.1038/nmat1080.
URL <http://www.ncbi.nlm.nih.gov/pubmed/14991018>
- [18] J. Wang, J. B. Neaton, H. Zheng, V. Nagarajan, S. B. Ogale, B. Liu, D. Viehland, V. Vaithyanathan, D. G. Schlom, U. V. Waghmare, N. a. Spaldin, K. M. Rabe, M. Wuttig, R. Ramesh, Epitaxial BiFeO₃ multiferroic thin film heterostructures., *Science (New York, N.Y.)* 299 (5613) (2003) 1719–22. doi:10.1126/science.1080615.
URL <http://www.ncbi.nlm.nih.gov/pubmed/12637741>
- [19] T. Zhao, A. Scholl, F. Zavaliche, K. Lee, M. Barry, A. Doran, M. P. Cruz, Y. H. Chu, C. Ederer, N. a. Spaldin, R. R. Das, D. M. Kim, S. H. Baek,

- C. B. Eom, R. Ramesh, Electrical control of antiferromagnetic domains in multiferroic BiFeO₃ films at room temperature., *Nature materials* 5 (10) (2006) 823–9. doi:10.1038/nmat1731.
URL <http://www.ncbi.nlm.nih.gov/pubmed/16951676>
- [20] C. Nan, Magnetoelectric effect in composites of piezoelectric and piezomagnetic phases, *Physical Review B* 50 (9) (1994) 6082.
URL http://prb.aps.org/abstract/PRB/v50/i9/p6082_1
- [21] J. Ryu, S. Priya, K. Uchino, H. Kim, Magnetoelectric effect in composites of magnetostrictive and piezoelectric materials, *Journal of Electroceramics* 8 (2) (2002) 107–119.
URL <http://www.springerlink.com/index/R26596P34UTL273X.pdf>
- [22] C.-W. Nan, M. I. Bichurin, S. Dong, D. Viehland, G. Srinivasan, Multiferroic magnetoelectric composites: Historical perspective, status, and future directions, *Journal of Applied Physics* 103 (3) (2008) 031101. doi:10.1063/1.2836410.
- [23] G. V. Duong, R. Groessinger, R. S. Turtelli, Magnetoelectric Properties of CoFe₂O₄ -BaTiO₃ Core-Shell Structure Composite, *IEEE Transactions on Magnetics* 42 (10) (2006) 3611–3613.
- [24] S. Dong, J. Zhai, J. Li, D. Viehland, Near-ideal magnetoelectricity in high-permeability magnetostrictive/piezofiber laminates with a (2-1) connectivity, *Applied Physics Letters* 89 (25) (2006) 252904. doi:10.1063/1.2420772.
- [25] R. a. Islam, Y. Ni, A. G. Khachaturyan, S. Priya, Giant magnetoelectric effect in sintered multilayered composite structures, *Journal of Applied Physics* 104 (4) (2008) 044103. doi:10.1063/1.2966597.
URL <http://link.aip.org/link/JAPIAU/v104/i4/p044103/s1&Agg=doi>
- [26] J.-g. Wan, H. Zhang, X. Wang, D. Pan, J.-m. Liu, G. Wang, Magnetoelectric CoFe₂O₄-lead zirconate titanate thick films prepared by a polyvinylpyrrolidone-assisted sol-gel method, *Applied Physics Letters* 89 (12) (2006) 122914. doi:10.1063/1.2357589.

- [27] H. Zheng, J. Wang, S. E. Lofland, Z. Ma, L. Mohaddes-Ardabili, T. Zhao, L. Salamanca-Riba, S. R. Shinde, S. B. Ogale, F. Bai, D. Viehland, Y. Jia, D. G. Schlom, M. Wuttig, a. Roytburd, R. Ramesh, Multiferroic BaTiO₃-CoFe₂O₄ Nanostructures., *Science* (New York, N.Y.) 303 (5658) (2004) 661–3. doi:10.1126/science.1094207.
URL <http://www.ncbi.nlm.nih.gov/pubmed/14752158>
- [28] C. Deng, Y. Zhang, J. Ma, Y. Lin, C.-W. Nan, Magnetoelectric effect in multiferroic heteroepitaxial BaTiO₃-NiFe₂O₄ composite thin films, *Acta Materialia* 56 (3) (2008) 405–412. doi:10.1016/j.actamat.2007.10.004.
URL <http://linkinghub.elsevier.com/retrieve/pii/S1359645407006684>
- [29] J. G. Wan, X. W. Wang, Y. J. Wu, M. Zeng, Y. Wang, H. Jiang, W. Q. Zhou, G. H. Wang, J.-M. Liu, Magnetoelectric CoFe₂O₄-Pb(Zr,Ti)O₃ composite thin films derived by a sol-gel process, *Applied Physics Letters* 86 (12) (2005) 122501. doi:10.1063/1.1889237.
- [30] F. Zavaliche, H. Zheng, L. Mohaddes-Ardabili, S. Y. Yang, Q. Zhan, P. Shafer, E. Reilly, R. Chopdekar, Y. Jia, P. Wright, D. G. Schlom, Y. Suzuki, R. Ramesh, Electric field-induced magnetization switching in epitaxial columnar nanostructures., *Nano letters* 5 (9) (2005) 1793–6. doi:10.1021/nl051406i.
URL <http://www.ncbi.nlm.nih.gov/pubmed/16159226>
- [31] S. Dong, J. Zhai, F. Bai, J.-F. Li, D. Viehland, Push-pull mode magnetostrictive/piezoelectric laminate composite with an enhanced magnetoelectric voltage coefficient, *Applied Physics Letters* 87 (6) (2005) 062502. doi:10.1063/1.2007868.
- [32] C. Israel, N. D. Mathur, J. F. Scott, A one-cent room-temperature magnetoelectric sensor 7 (February) (2008) 93–94.
- [33] J. Yang, Y. Wen, P. Li, X. Dai, A magnetoelectric, broadband vibration-powered generator for intelligent sensor systems, *Sensors and Actuators A: Physical* 168 (2) (2011) 358–364. doi:10.1016/j.sna.2011.04.038.
URL <http://linkinghub.elsevier.com/retrieve/pii/S0924424711002858>

- [34] X. Dai, Y. Wen, P. Li, J. Yang, M. Li, Energy harvesting from mechanical vibrations using multiple magnetostrictive/piezoelectric composite transducers, *Sensors and Actuators A: Physical* 166 (1) (2011) 94–101. doi:10.1016/j.sna.2010.12.025.
URL <http://linkinghub.elsevier.com/retrieve/pii/S0924424711000021>
- [35] S. Dong, J. F. Li, D. Viehland, J. Cheng, L. E. Cross, A strong magnetoelectric voltage gain effect in magnetostrictive-piezoelectric composite, *Applied Physics Letters* 85 (16) (2004) 3534. doi:10.1063/1.1786631.
- [36] S. Dong, J.-F. Li, D. Viehland, Magnetoelectric coupling, efficiency, and voltage gain effect in piezoelectric-piezomagnetic laminate composites, *Journal of Materials Science* 41 (1) (2006) 97–106. doi:10.1007/s10853-005-5930-8.
- [37] M. Bichurin, V. Petrov, Y. Kiliba, G. Srinivasan, Magnetic and magnetoelectric susceptibilities of a ferroelectric/ferromagnetic composite at microwave frequencies, *Physical Review B* 66 (2002) 134404. doi:10.1103/PhysRevB.66.134404.
URL <http://link.aps.org/doi/10.1103/PhysRevB.66.134404>
- [38] Y. K. Fetisov, G. Srinivasan, Electric field tuning characteristics of a ferrite-piezoelectric microwave resonator, *Applied Physics Letters* 88 (14) (2006) 143503. doi:10.1063/1.2191950.
URL <http://link.aip.org/link/APPLAB/v88/i14/p143503/s1&Agg=doi>
- [39] J. F. Scott, Applications of modern ferroelectrics., *Science* (New York, N.Y.) 315 (5814) (2007) 954–9. doi:10.1126/science.1129564.
URL <http://www.ncbi.nlm.nih.gov/pubmed/17303745>
- [40] Y.-H. Chu, L. W. Martin, M. B. Holcomb, M. Gajek, S.-J. Han, Q. He, N. Balke, C.-H. Yang, D. Lee, W. Hu, Q. Zhan, P.-L. Yang, A. Fraile-Rodríguez, A. Scholl, S. X. Wang, R. Ramesh, Electric-field control of local ferromagnetism using a magnetoelectric multiferroic., *Nature materials* 7 (6) (2008) 478–82. doi:10.1038/nmat2184.
URL <http://www.ncbi.nlm.nih.gov/pubmed/18438412>

- [41] M. Bibes, Towards a magnetoelectric memory, *Nature materials* 7 (6) (2008) 425–426.
- [42] R. Singh, T. Bhimasankaram, G. Kumar, S. Suryanarayana, Dielectric and magnetoelectric properties of $\text{Bi}_5\text{FeTi}_3\text{O}_{15}$, *Solid State Communications* 91 (7) (1994) 567–569.
- [43] J.-P. Rivera, On definitions, units, measurements, tensor forms of the linear magnetoelectric effect and on a new dynamic method applied to Cr-Cl boracite, *Ferroelectrics* 161 (1994) 165–180.
- [44] G. V. Duong, R. Groessinger, M. Schoenhardt, D. Bueno-Basques, The lock-in technique for studying magnetoelectric effect, *Journal of Magnetism and Magnetic Materials* 316 (2) (2007) 390–393. doi:10.1016/j.jmmm.2007.03.185.
URL <http://linkinghub.elsevier.com/retrieve/pii/S0304885307003770>
- [45] J. Y. Zhai, N. Cai, L. Liu, Y. H. Lin, C. W. Nan, Dielectric behavior and magnetoelectric properties of lead zirconate titanate/Co-ferrite particulate composites, *Materials Science and Engineering: B* 99 (1-3) (2003) 329–331. doi:10.1016/S0921-5107(02)00565-2.
URL <http://linkinghub.elsevier.com/retrieve/pii/S0921510702005652>
- [46] G. V. Duong, R. S. Turtelli, R. Groessinger, Magnetoelectric properties of $\text{CoFe}_2\text{O}_4\text{-BaTiO}_3$ core-shell structure composite studied by a magnetic pulse method, *Journal of Magnetism and Magnetic Materials* 322 (9-12) (2010) 1581–1584. doi:10.1016/j.jmmm.2009.09.022.
URL <http://linkinghub.elsevier.com/retrieve/pii/S0304885309009226>
- [47] M. E. Botello-Zubiate, D. Bueno-Baqués, J. De Frutos Vaquerizo, L. E. Fuentes Cobas, J. a. Matutes-Aquino, Magnetoelectric Measurements by Two Different Methods of Cobalt Ferrite-Barium Titanate Composites, *Ferroelectrics* 338 (1) (2006) 247–253. doi:10.1080/00150190600740374.
URL <http://www.tandfonline.com/doi/abs/10.1080/00150190600740374>
- [48] Y. Fetisov, K. Kamentsev, a.Y. Ostashchenko, G. Srinivasan, Wide-band magnetoelectric characterization of a ferrite-piezoelectric multilayer

- using a pulsed magnetic field, *Solid State Communications* 132 (1) (2004) 13–17. doi:10.1016/j.ssc.2004.07.019.
URL <http://linkinghub.elsevier.com/retrieve/pii/S0038109804005642>
- [49] M. Vopsaroiu, M. Stewart, T. Hegarty, A. Muniz-Piniella, N. McCartney, M. Cain, G. Srinivasan, Experimental determination of the magnetoelectric coupling coefficient via piezoelectric measurements, *Measurement Science and Technology* 19 (4) (2008) 045106. doi:10.1088/0957-0233/19/4/045106.
- [50] L. Yan, Z. Xing, Z. Wang, T. Wang, G. Lei, J. Li, D. Viehland, Direct measurement of magnetoelectric exchange in self-assembled epitaxial BiFeO₃-CoFe₂O₄ nanocomposite thin films, *Applied Physics Letters* 94 (19) (2009) 192902. doi:10.1063/1.3138138.
URL <http://link.aip.org/link/APPLAB/v94/i19/p192902/s1&Agg=doi>
- [51] P. Borisov, a. Hochstrat, V. V. Shvartsman, W. Kleemann, Superconducting quantum interference device setup for magnetoelectric measurements., *The Review of scientific instruments* 78 (10) (2007) 106105. doi:10.1063/1.2793500.
URL <http://www.ncbi.nlm.nih.gov/pubmed/17979461>
- [52] S. Bhame, P. Joy, Enhanced magnetostrictive properties of CoFe₂O₄ synthesized by an autocombustion method, *Sensors and Actuators A: Physical* 137 (2) (2007) 256–261. doi:10.1016/j.sna.2007.03.016.
URL <http://linkinghub.elsevier.com/retrieve/pii/S0924424707001938>
- [53] C. Cannas, a. Falqui, a. Musinu, D. Peddis, G. Piccaluga, CoFe₂O₄ nanocrystalline powders prepared by citrate-gel methods: Synthesis, structure and magnetic properties, *Journal of Nanoparticle Research* 8 (2) (2006) 255–267. doi:10.1007/s11051-005-9028-7.
URL <http://www.springerlink.com/index/10.1007/s11051-005-9028-7>
- [54] V. Corral-Flores, D. Bueno-Baques, D. Carrillo-Flores, J. a. Matutes-Aquino, Enhanced magnetoelectric effect in core-shell particulate composites, *Journal of Applied Physics* 99 (8) (2006) 08J503.

- doi:10.1063/1.2165147.
URL <http://link.aip.org/link/JAPIAU/v99/i8/p08J503/s1&Agg=doi>
- [55] V. Corral-Flores, D. Bueno-Baqués, R. Ziolo, Synthesis and characterization of novel $\text{CoFe}_2\text{O}_4\text{-BaTiO}_3$ multiferroic core-shell-type nanostructures, *Acta Materialia* 58 (3) (2010) 764–769. doi:10.1016/j.actamat.2009.09.054.
URL <http://linkinghub.elsevier.com/retrieve/pii/S1359645409006600>
- [56] C. Ciomaga, C. Galassi, F. Prihor, I. Dumitru, L. Mitoseriu, A. Iordan, M. Airimioaei, M. Palamaru, Preparation and properties of the $\text{CoFe}_2\text{O}_4\text{-Nb-Pb(Zr,Ti)O}_3$ multiferroic composites prepared in situ by gel-combustion method, *Journal of Alloys and Compounds* 485 (1-2) (2009) 372–378. doi:10.1016/j.jallcom.2009.05.101.
URL <http://linkinghub.elsevier.com/retrieve/pii/S0925838809010810>
- [57] a.R. Iordan, M. Airimioaei, M. Palamaru, C. Galassi, A. Sandu, C. Ciomaga, F. Prihor, L. Mitoseriu, A. Ianculescu, In situ preparation of $\text{CoFe}_2\text{O}_4\text{-Pb(ZrTi)O}_3$ multiferroic composites by gel-combustion technique, *Journal of the European Ceramic Society* 29 (13) (2009) 2807–2813. doi:10.1016/j.jeurceramsoc.2009.03.031.
URL <http://linkinghub.elsevier.com/retrieve/pii/S0955221909001460>
- [58] A. Muhammad, Development and Investigation of New Magnetoelectric Composites, Ph.D. thesis, Vienna University of Technology (2011).
- [59] R. Groessinger, Characterization of Hard Magnetic Materials, *Journal of Electrical Engineering* 59 (7) (2008) 15–20.
- [60] <http://www.vishaypg.com>.
URL www.vishaypg.com
- [61] <http://www.hbm.com>.
URL <http://www.hbm.com>
- [62] A. Muhammad, Development and Investigation of New Magnetoelectric Composites, Ph.D. thesis, Vienna University of Technology (2011).

- [63] C. A. Randall, N. Kim, J.-p. Kucera, W. Cao, T. R. Shrout, Intrinsic and Extrinsic Size Effects in Fine-Grained Morphotropic-Phase-Boundary Lead Zirconate Titanate Ceramics, *Journal of American Ceramic Society* 81 (3) (1998) 677–688.
- [64] M. Ghasemifard, S. Hosseini, a. Khorsand Zak, G. H. Khorrami, Microstructural and optical characterization of PZT nanopowder prepared at low temperature, *Physica E: Low-dimensional Systems and Nanostructures* 41 (3) (2009) 418–422. doi:10.1016/j.physe.2008.09.017.
URL <http://linkinghub.elsevier.com/retrieve/pii/S1386947708003585>
- [65] R. Grössinger, G. V. Duong, R. Sato-Turtelli, The physics of magnetoelectric composites, *Journal of Magnetism and Magnetic Materials* 320 (14) (2008) 1972–1977. doi:10.1016/j.jmmm.2008.02.031.
URL <http://linkinghub.elsevier.com/retrieve/pii/S0304885308001212>
- [66] A. Muhammad, Development and Investigation of New Magnetoelectric Composites, Ph.D. thesis, TU Vienna (2011).
- [67] A. Muhammad, R. Sato-Turtelli, M. Kriegisch, R. Groessinger, F. Kubel, T. Konegger, Large enhancement of magnetostriction due to compaction hydrostatic pressure and magnetic annealing in CoFe_2O_4 , *Journal of Applied Physics* 111 (1) (2012) 013918. doi:10.1063/1.3675489.
URL <http://link.aip.org/link/JAPIAU/v111/i1/p013918/s1&Agg=doi>
- [68] A. Muhammad, Development and Investigation of New Magnetoelectric Composites, Ph.D. thesis (2011).